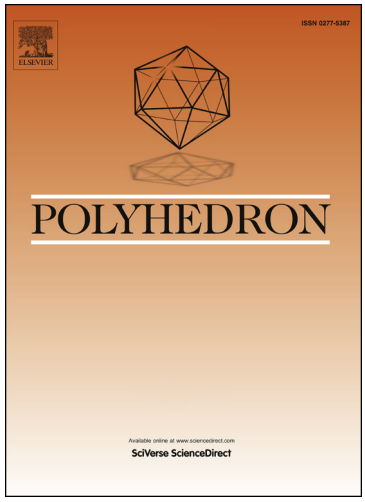

Synthesis, characterization and catalytic activity of dioxidomolybdenum(VI) complexes of tribasic pentadentate ligands

Mannar R. Maurya, Sarita Dhaka, Fernando Avecilla

PII: S0277-5387(13)00613-X
DOI: http://dx.doi.org/10.1016/j.poly.2013.08.050
Reference: POLY 10310

To appear in: *Polyhedron*

Received Date: 12 June 2013
Accepted Date: 4 August 2013

Please cite this article as: M.R. Maurya, S. Dhaka, F. Avecilla, Synthesis, characterization and catalytic activity of dioxidomolybdenum(VI) complexes of tribasic pentadentate ligands, *Polyhedron* (2013), doi: http://dx.doi.org/10.1016/j.poly.2013.08.050

(Graphical Abstract)

Synthesis, characterization and catalytic activity of dioxidomolybdenum(VI) complexes of tribasic pentadentate ligands

M. R. Maurya, S. Dhaka, F. Avecilla

Dioxidomolybdenum(VI) complexes of tribasic pentadentate ligands have been isolated and characterized. Their catalytic activities for the oxidative bromination of styrene and the oxidation of methyl phenyl sulfide and benzoin are reported.

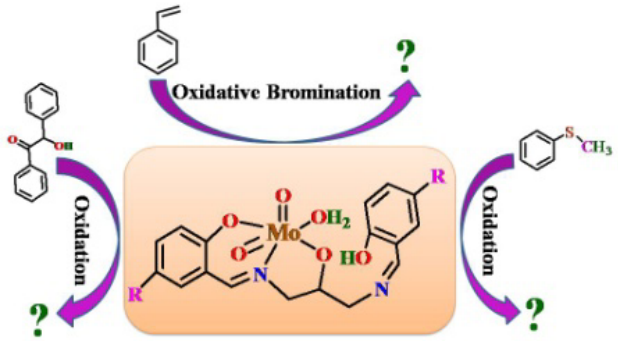

Synthesis, characterization and catalytic activity of dioxidomolybdenum(VI) complexes of tribasic pentadentate ligands

M. R. Maurya, S. Dhaka, F. Avecilla

Research Highlights

1. Dioxidomolybdenum(VI) complexes of tribasic pentadentate ligands are reported.
2. The ligands behave only as a dibasic tridentate ONO donor in these complexes.
3. These complexes present functional models of vanadium dependent haloperoxidases.
4. These complexes catalyze the oxidative bromination of styrene and the oxidation of methyl phenyl sulfide and benzoin.

Synthesis, characterization and catalytic activity of dioxidomolybdenum(VI) complexes of tribasic pentadentate ligands

Mannar R. Maurya,[a,*] Sarita Dhaka,[a] Fernando Avecilla[b]

[a]*Department of Chemistry, Indian Institute of Technology Roorkee, Roorkee 247 667, India.*
[b]*Departamento de Química Fundamental, Universidade da Coruña, Campus de A Zapateira, 15071 A Coruña, Spain*

Keywords: Mo complexes; NMR spectroscopy; Crystal structure; Oxidative bromination of styrene; Oxidation of methyl phenyl sulfide; Oxidation of benzoin.

---

* To whom correspondence should be addressed. E. mail: rkmanfcy@iitr.ernet.in (M.R. Maurya), Tel: +91 1332 285327. Fax: +91 1332 273560.

Abstract

$[Mo^{VI}O_2(acac)_2]$ (Hacac = acetylacetone) reacts with the tribasic pentadentate Schiff bases H_3sal-dahp (**I**), H_3clsal-dahp (**II**) and H_3brsal-dahp (**III**) (sal = salicylaldehyde, clsal = 5-chlorosalicylaldehyde, brsal = 5-bromosalicylaldehyde, dahp = 1,3-diamino-2-hydroxypropane) in methanol under refluxing conditions to yield the dioxidomolybdenum(VI) complexes $[Mo^{VI}O_2(Hsal\text{-}dahp)(H_2O)]$ (**1**), $[Mo^{VI}O_2(Hclsal\text{-}dahp)(H_2O)]$ (**2**) and $[Mo^{VI}O_2(Hbrsal\text{-}dahp)(H_2O)]$ (**3**), respectively. In these complexes, only one set of phenolic oxygen and azomethine nitrogen atoms, along with the alcoholic oxygen atom of the ligands coordinate to the molybdenum. The reactions of these complexes with pyridine result in the formation of $[Mo^{VI}O_2(Hsal\text{-}dahp)(py)]$ (**4**), $[Mo^{VI}O_2(Hclsal\text{-}dahp)(py)]$ (**5**) and $[Mo^{VI}O_2(Hbrsal\text{-}dahp)(py)]$ (**6**). A single crystal X-ray study of $[Mo^{VI}O_2(Hbrsal\text{-}dahp)(DMSO)]$ (**3a**), grown by slow evaporation of a DMSO solution of **3**, confirms the non-participation of one set of phenolic oxygen and azomethine nitrogen atoms of the ligand. The reaction of a methanolic solution of the in-situ generated H_3clsal-dahp with $[Mo^{VI}O_2(acac)_2]$ in DMSO gave $[Mo^{VI}O_2(Hclsal\text{-}hdap)(DMSO)]_4[Mo_8O_{26}]\cdot 6DMSO$ (**7**) (H_2clsal-hdap = Schiff base obtained by the 1:1 condensation of 5-chlorosalicylaldehyde and 1,3-diamino-2-hydroxypropane), where the non-coordinated azomethine nitrogen hydrolyzes giving a free protonated amine group, as confirmed by a single crystal X-ray study. Complexes **1**, **2** and **3** catalyze the oxidative bromination of styrene to yield 1,2-dibromo-1-phenyl-ethane, 1-phenylethane-1,2-diol and 2-bromo-1-phenylethane-1-ol; therefore they act as functional models of vanadium dependent haloperoxidases. It has also been demonstrated that complexes **1**, **2** and **3** are catalyst precursors for the oxidation of methyl phenyl sulfide and benzoin.

1. Introduction

The significant enzymatic role of molybdenum in biochemical reactions, especially in the oxidation of aldehydes, purines and sulfides [1,2], has attracted researchers to use high-valent molybdenum complexes with a cis-$[Mo^{VI}O_2]$ functionality as biomimetic catalysts in the oxygenation of organic compounds [3-5]. The oxygen atom transfer properties of these complexes play a significant role in investigating the functioning mechanism of molybdenum

transferase enzymes, which also consist of a cis-[$Mo^{VI}O_2$] moiety as the active site [6-12]. The tendency of molybdenum to form stable complexes with oxygen, nitrogen and sulfur donor containing ligands has led to the development of high-valent molybdenum Schiff base complexes which are effective catalysts both in homogeneous and heterogeneous reactions [13-27]. The performance of these complexes varies noticeably with the nature of the ligands and the available coordination sites [13-27].

Ligands derived from 1,3-diamino-2-hydroxypropane and salicylaldehyde, substituted salicylaldehyde (H_3xsal-dahp, Scheme 1) or *o*-hydroxyacetophenone are tribasic pentadenate ligands with good flexibility. However, the participation or non-participation of the alcoholic hydroxyl group and of a second Schiff base moiety may results in interesting tridentate, tetradentate and pentadentate coordinating behavior of these ligands [28,29]. In fact, dibasic tetradentate and tribasic pentadentate behaviours of these ligands have been confirmed in oxidovanadium(IV) and oxidovanadium(V) complexes, respectively. Further, the vanadium complex [V^{IV}O(Hsal-dahp)], in which the alcoholic oxygen atom of the amine residue does not participate in coordination, undergoes decomposition under aerobic atmosphere at reflux temperature in methanol producing a new dioxidovanadium(V) complex where hydrolysis of the azomethine nitrogen occurs, giving a free amino group along with the loss of the salicylaldehyde moiety; here the alcoholic oxygen also coordinates after proton replacement and the new ligand behaves as a dibasic tridentate ONO system [28].

A recent review by Chakravarthy and Chand gives an account of the synthetic strategies of several cis-$[Mo^{VI}O_2]^{2+}$ complexes of dianionic tridentate ONO ligands [30]. Catalytic applications of molybdenum complexes in organic transformations [13-27,31-36] and oxidation of sulfides [37-39] have also been explored, while oxidative bromination of organic substrates, a reaction normally promoted by vanadium haloperoxidase enzymes [40-42], has rarely been studied [32,43].

The interesting behavior of H_3xsal-dahp [28,29] and wide catalytic applications of molybdenum complexes prompted us to undertake the synthesis and characterization of new dioxidomolybdenum(VI) complexes of H_3xsal-dahp. Their catalytic potentials are demonstrated

by studying the oxidative bromination of styrene and the oxidation of methyl phenyl sulfide. In addition, the oxidation of benzoin by peroxide has also been reported.

<<Scheme 1>>

2. Experimental section

2.1. Materials

Ammonium molybdate (Loba Chemie, India), 1,3-diamino-2-hydroxypropane (Hdahp), acetylacetone (Hacac) (Aldrich, U.S.A.), salicylaldehyde (Sisco research, India), methyl phenyl sulfide (Alfa Aesar, U.S.A.), styrene (Acros Organics, U.S.A.), benzoin (S.D. Fine, India), 70 % aqueous $HClO_4$ and 30% aqueous H_2O_2 (Qualigens, India) were used as obtained. All other chemicals and solvents used were of AR grade. $[Mo^{VI}O_2(acac)_2]$ was prepared according to the method reported in the literature [44].

2.2. Instrumentation and characterization procedures

Elemental analyses of the ligands and complexes were obtained by an Elementar model Vario-EL-III. IR spectra were recorded as KBr pellets on a Nicolet 1100 FT-IR spectrometer after grinding the sample with KBr. Electronic spectra of the ligand and complexes were recorded in methanol or DMSO using a Shimadzu 1601 UV-vis spectrophotometer. ^1H NMR spectra were recorded on a Bruker Avance 500 MHz spectrometer with the common parameter settings in DMSO-d_6. The δ values are quoted relative to TMS as an internal standard. Thermogravimetric analyses of the complexes were carried out using a Perkin Elmer (Pyris Diamond) instrument in air with a heating rate of 10 ^oC/ min. A Shimadzu Nicolet gas chromatograph with a HP–1 capillary column (30 m × 0.25 mm × 0.25 μm) was used to analyze the reaction products. The identity of the products was confirmed using a GC-MS model Perkin-Elmer, Clarus 500 by comparing the fragments of each product with the library available. The percent conversion of substrate and selectivity of products were calculated from GC data using the formulae presented elsewhere [45].

2.3. X-ray crystal structure determination

Three-dimensional room temperature X-ray data were collected on a Bruker Kappa Apex CCD diffractometer at low temperature for **3a** and **7** by the ϕ-ω scan method. Reflections were measured from a hemisphere of data collected from frames, each of them covering 0.3º in ω. Of the 31885 reflections measured for **3a** and 81546 for **7**, all were corrected for Lorentz and polarization effects and for absorption by multi-scan methods based on symmetry-equivalent and repeated reflections, 3724 and 10219 independent reflections, respectively, exceeded the significance level ($|F|/\sigma|F|$) > 4.0. Complex scattering factors were taken from the program package SHELXTL [46]. The structures were solved by direct methods and refined by full matrix least-squares on F^2. Hydrogen atoms were included in calculated positions and refined in the riding mode. Refinements were done with allowance for thermal anisotropy of all non-hydrogen atoms. Further details of the crystal structure determinations are given in Table 1.

<<<Table 1>>

2.4. Preparation

*2.4.1. Preparation of H_3sal-dahp (**I**), H_3clsal-dahp (**II**) and H_3brsal-dahp (**III**)*

The ligand H_3sal-dahp was prepared as reported previously [28]. The other ligands were prepared following essentially same procedure.

*Data for H_3sal-dahp (**I**):* Yield 5.36 g (90%). Anal. Calc. for $C_{17}H_{18}N_2O_3$ (298.34): C, 68.41; H, 6.13; N, 9.48. Found: C, 68.05; H, 6.02; N, 9.50% .

*Data for H_3clsal-dahp (**II**):* Yield: 3.27 g (89%). Anal. Calc. for $C_{17}H_{16}N_2O_3Cl_2$ (367.23): C, 55.69; H, 4.43; N, 7.63. Found: C, 55.60; H, 4.26; N, 7.58 %.

*Data for H_3brsal-dahp (**III**):* Yield: 4.10 g (90%). Anal. Calc. for $C_{17}H_{16}N_2O_3Br_2$ (456.13): C, 44.76; H, 3.54; N, 6.14. Found: C, 44.69; H, 3.36; N, 6.07%.

*2.4.2. Preparation of [$Mo^{VI}O_2$(Hsal-dahp)(H_2O)] (**1**)*

A stirred solution of H_3sal-dahp (0.60 g, 2 mmol) in methanol (10 mL) was treated with [$Mo^{VI}O_2(acac)_2$] (0.66 g, 2 mmol) dissolved in methanol (10 mL) and the obtained reaction mixture was stirred, whereupon an yellow solid started to form immediately. After 1 h of stirring,

the separated solid was filtered, washed with methanol and dried in a vacuum desiccator over silica gel. Yield: 0.643 g (75%). Anal. Calc. for $C_{17}H_{18}N_2O_6Mo$ (444): C, 45.94; H, 4.09; N, 6.31. Found: C, 45.86; H, 4.05; N, 6.27 %.

*2.4.3. Preparation of [$Mo^{VI}O_2$(Hclsal-dahp)(H_2O)] (**2**)*

Complex **2** was prepared from [$MoO_2{}^{VI}$ $(acac)_2$] (0.66 g, 2 mmol) and H_3clsal-dahp (0.73 g, 2 mmol) by the method outlined for **1**. The separated solid was filtered, washed with methanol and dried in a vacuum desiccator over silica gel. Yield: 0.745 g (75%). Anal. Calc. for $C_{17}H_{16}N_2O_6Cl_2Mo$ (512): C, 39.85; H, 3.15; N, 5.47. Found: C, 39.68; H, 3.21; N, 5.38 %.

*2.4.4. Preparation of [$Mo^{VI}O_2$(Hbrsal-dahp)(H_2O)] (**3**)*

This complex was prepared by the procedure outlined for **1**, using [$MoO_2{}^{VI}$ $(acac)_2$] (0.66 g, 2 mmol) and H_3brsal-dahp (0.912 g, 2 mmol). The separated solid was filtered, washed with methanol and dried in a vacuum desiccator over silica gel. Yield: 1.075 g (92%). Anal. Calc. for $C_{17}H_{16}N_2O_6Br_2Mo$ (599.8): C, 34.01; H, 2.69; N, 4.67. Found: C, 33.92; H, 2.62; N, 4.53 %. Crystals of [$Mo^{VI}O_2$(Hbrsal-dahp)(DMSO)] (**3a**) were grown by slow evaporation of a solution of **3** in DMSO.

*2.4.5. Preparation of [$Mo^{VI}O_2$(Hsal-dahp)(py)] (**4**), [$Mo^{VI}O_2$(Hclsal-dahp)(py)] (**5**) and [$Mo^{VI}O_2$(Hbrsal-dahp)(py)] (**6**)*

Complexes [$Mo^{VI}O_2$(Hsal-dahp)(H_2O)] (**1**), [$Mo^{VI}O_2$(Hclsal-dahp)(H_2O)] (**2**) and [$Mo^{VI}O_2$(Hbrsal-dahp)(H_2O)] (**3**) (1 mmol each) were dissolved in a minimum amount of pyridine and evaporated slowly under vacuum whereupon a yellow solid in each case slowly precipitated. These were filtered, washed with methanol and dried in a vacuum desiccator over silica gel. A nearly quantitative yield was obtained in all cases.

*Data for [$Mo^{VI}O_2$(Hsal-dahp)(py)] (**4**):* Anal. Calc. for $C_{22}H_{21}N_3O_5Mo$ (503): C, 56.06; H, 4.49; N, 8.91. Found: C, 56.52; H, 4.78; N, 9.03 %.

*Data for [$Mo^{VI}O_2$(Hclsal-dahp)(py)] (**5**):* Anal. Calc. for $C_{22}H_{19}N_3O_5Cl_2Mo$ (572.26): C, 48.94; H, 3.54; N, 7.78. Found: C, 48.56; H, 3.62; N, 7.59 %.

*Data for [$Mo^{VI}O_2$(Hbrsal-dahp)(py)] (**6**):* Anal. Calc. for $C_{22}H_{19}N_3O_5Br_2Mo$ (661.16): C, 42.09; H, 3.04; N, 6.68. Found: C, 42.41; H, 3.12; N, 6.80 %.

*2.4.6. Preparation of [$Mo^{VI}O_2$(Hclsal-hdap)(DMSO)]$_4$[Mo_8O_{26}]·6DMSO (**7**)*

Salicylaldehyde (0.244 g, 2 mmol) and 1,3-diamino-2-hydroxypropane (0.090 g, 1 mmol) were taken in methanol (20 mL) and refluxed for 2 h. A solution of [$Mo^{VI}O_2(acac)_2$] (0.33 g, 1 mmol) in DMSO (10 mL) was added to the above solution and the reaction mixture was heated at 80 ^oC for 1 h and then kept at room temperature for slow evaporation. After a few days, the obtained yellow crystals were filtered and dried in air. No satisfactory elemental analyses could be obtained.

2.5. Catalytic activity studies

The complexes [$Mo^{VI}O_2$(Hsal-dahp)(H_2O)] (**1**), [$Mo^{VI}O_2$(Hclsal-dahp)(H_2O)] (**2**) and [$Mo^{VI}O_2$(Hbrsal-dahp)(H_2O)] (**3**) were used as catalysts for the oxidative bromination of styrene and the oxidation of methyl phenyl sulfide and benzoin. All reactions were carried out in a 50 mL two necked glass reaction flask fitted with a water circulated condenser.

2.5.1. Oxidative bromination of styrene

Styrene (1.04 g, 10 mmol), 30 % aqueous H_2O_2 (2.27 g, 20 mmol), 70% $HClO_4$ (4.29 g, 30 mmol) and KBr (2.38 g, 20 mmol) were taken in a mixture of dichloromethane-water (40 mL, V/V) at room temperature. After adding the catalyst (0.001g) to the above reaction mixture, it was stirred and the obtained oxidized products were analyzed quantitatively by gas chromatography by withdrawing small aliquots of the reaction mixture present in the CH_2Cl_2 layer at 15 minute intervals. The identities of the products were confirmed by GC-MS and their quantifications were made on the basis of the relative peak area of the respective product.

2.5.2. Oxidation of methyl phenyl sulfide

Methyl phenyl sulfide (1.24 g, 10 mmol), 30 % aqueous H_2O_2 (2.27 g, 20 mmol) and catalyst (0.0015 g) were mixed in acetonitrile (5 mL) and stirred at room temperature. The reaction was monitored by withdrawing small aliquots of the reaction mixture every 30 minutes and analyzing them quantitatively by gas chromatography. The identities of the products were confirmed by GC–MS. The effects of various parameters, such as amounts of oxidant, catalyst and solvent, were studied to see their effects on the conversion and selectivity of the reaction products.

2.5.3. Oxidation of benzoin

Benzoin (1.06 g, 5 mmol), 30 % aqueous H_2O_2 (1.69 g, 15 mmol) and catalyst (0.0005 g) were mixed in methanol (10 mL) and the reaction was carried out at the reflux temperature of methanol. The reaction was monitored by withdrawing small aliquots of the reaction mixture every 60 minutes and analyzing them quantitatively by gas chromatography. The identities of the products were confirmed by GC–MS. The effects of various parameters, such as amounts of oxidant, catalyst and solvent, were studied to see their effects on the conversion and selectivity of the reaction products.

3. Results and discussion

3.1. Synthesis and characterization of the complexes

The reaction between equimolar amounts of $[Mo^{VI}O_2(acac)_2]$ (Hacac = acetylacetone) and the ligands H_3sal-dahp (**I**), H_3clsal-dahp (**II**) and H_3brsal-dahp (**III**) in refluxing methanol leads to the formation of the dioxidomolybdenum(VI) complexes $[Mo^{VI}O_2(Hsal\text{-}dahp)(H_2O)]$ (**1**), $[Mo^{VI}O_2(Hclsal\text{-}dahp)(H_2O)]$ (**2**) and $[Mo^{VI}O_2(Hbrsal\text{-}dahp)(H_2O)]$ (**3**), respectively [Eq. (1) taking H_3sal-dahp (**I**) as a representative example].

$$[Mo^{VI}O_2(acac)_2] + H_3\text{sal-dahp} + H_2O \rightarrow [Mo^{VI}O_2(Hsal\text{-}dahp)(H_2O)] + 2Hacac \quad (1)$$

All these complexes possibly exist as monomers [43,48] and are soluble in DMSO and DMF only. Complexes **1**-**3** also dissolve in pyridine, giving $[Mo^{VI}O_2(Hsal\text{-}dahp)(py)]$ (**4**), $[Mo^{VI}O_2(Hclsal\text{-}dahp)(py)]$ (**5**) and $[Mo^{VI}O_2(Hbrsal\text{-}dahp)(py)]$ (**6**) (Eq. 2 considering $[Mo^{VI}O_2(Hsal\text{-}dahp)(H_2O)]$ as a representative example) where the pyridine ligand occupies the sixth coordination position in these complexes. The pyridine containing complexes are soluble in methanol, DMSO and DMF. The complex $[Mo^{VI}O_2(Hclsal\text{-}hdap)(DMSO)]_4[Mo_8O_{26}]\cdot 6DMSO$ (**7**), obtained by the reaction of $[Mo^{VI}O_2(acac)_2]$ dissolved in DMSO and in-situ generated H_3clsal-dahp in methanol, is of interest as one of the salicylaldehyde moieties is lost and the azomethine group is converted into an amine group upon hydrolysis followed by protonation. Part of the complex is also decomposed to give a molybdenum polyhedron as a side product. Scheme 2 provides idealized structures of the complexes, which are based on the spectroscopic (IR, UV/Vis, ^{1}H and ^{13}C NMR) data, elemental analyses and X-ray diffraction studies of **3a** and **7**.

$[Mo^{VI}O_2(Hsal\text{-}dahp)(H_2O)] + py \rightarrow [Mo^{VI}O_2(Hsal\text{-}dahp)(py)] + H_2O$ (2)

<<Scheme 2>>

3.2. Thermal studies

The dioxidomolybdenum(VI) complexes **1**, **2** and **3** lose weight equal to one water molecule [4.3 % (Calcd: 4.1 %) for **1**, 3.6 % (Calcd: 3.5 %) for **2** and 3.2 % (Calcd: 3.0 %) for **3**] in the temperature range 100-265 °C, indicative of covalently but not strongly bonded water. When water is coordinated in the *trans* position to one of the doubly bonded oxygen atoms (see the structure of **3a**), its weak bonding is expected (cf. Scheme 2). The anhydrous complexes decompose exothermically in two/three overlapping steps on further increase of the temperature and form MoO_3 at ca. 600 ^{o}C (for **1**), ca. 500 ^{o}C (for **2**) and at ca. 450 ^{o}C (for **3**) as the final product. The pyridine coordinated complexes are stable up to ca. 150 ^{o}C. The weight loss equivalent to one pyridine takes place between 150 and 200 ^{o}C in the first step. Above this temperature continuous exothermic decomposition of the complexes occurs until the formation of the respective metal trioxide, MoO_3 at ca. 600 ^{o}C (for **4**), ca. 480 ^{o}C (for **5**) and at ca. 450 ^{o}C

(for **6**). Decomposition of the ligands in these complexes in overlapping multiple steps did not allow the estimation of intermediates.

3.3. Structure descriptions

The ORTEP diagram, along with the atom labelling scheme, for [$Mo^{VI}O_2$(Hbrsal-dahp)(DMSO)] (**3a**) is shown in Fig. 1, while ORTEP diagrams for the cation [$Mo^{VI}O_2$(Hclsal-hdap)(DMSO)]$^+$ and anion $[Mo_8O_{26}]^{4-}$ of [$Mo^{VI}O_2$(Hclsal-hdap)(DMSO)]$_4$[Mo_8O_{26}]·6DMSO (**7**) are shown in Figs. 2 and 3, respectively. Selected bond distances and angles are given in Table 2. The complexes adopt a six-coordinated structure in a distorted octahedral geometry. In these complexes, the phenolic oxygen, alcoholic oxygen and azomethine nitrogen atoms of the ligands coordinate to the molybdenum. One DMSO molecule and two oxo groups complete the coordination sphere. In complex **3a**, the other phenolic oxygen and azomethine nitrogen atoms remain non-coordinated, while in the [$Mo^{VI}O_2$(Hclsal-hdap)(DMSO)]$^+$ cation of complex **7**, the non-coordinated moiety hydrolyzes at the azomethine nitrogen atom, giving a free amine group which exists in the protonated form.

The asymmetric unit of **7** contains two [$Mo^{VI}O_2$(Hclsal-hdap)(DMSO)]$^+$ complexes, half a $[Mo_8O_{26}]^{4-}$ anion, and three molecules of free DMSO. The whole formula is thus written as [$Mo^{VI}O_2$(Hclsal-hdap)(DMSO)]$_4$[Mo_8O_{26}]·6DMSO (see Fig. 4). One DMSO molecule is coordinated to the Mo atom of one of the complexes present in the asymmetric unit, showing a disorder on the sulfur and carbon atoms. Two atomic sites have been observed for this DMSO molecule [the site occupancy factor for C(1A), C(2A), S(1A) is 0.38347]. One coordinated oxygen atom of an oxo group presents a disorder in the same complex. Two atomic sites have been observed for this oxygen atom [the site occupancy factor for O(3C) is 0.36016]. The molecular geometry of the $[Mo_8O_{26}]^{4-}$ anions correspond to β isomers with C_{2h} symmetry. In this form, all Mo atoms are six-coordinated, but are not equivalent [49]. The oxygen sites can be included in four categories, terminal (O_t), two-coordinate (O_{2c}), three coordinate (O_{3c}) and five-coordinate (O_{5c}). Bond distances are given in Table 3 and are in agreement with those observed for other compounds containing the β-octamolybdate anion [49]. The O(15) atom constitutes a

special case because it has two different distances to a metal centre. It can be considered as a pseudo-terminal oxygen atom [50].

<<Figures 1, 2, 3 and 4>> <<Table 2 and 3>>

3.4. IR spectral studies

Fig. S1 of the supporting information presents the IR spectra of H_3sal-dahp (**I**) and [$Mo^{VI}O_2$(Hsal-dahp)(H_2O)] (**1**). The IR spectra of the ligands (Table 4) exhibit a sharp band due to the ν(C=N) (azomethine) stretch at 1633-1638 cm^{-1}. This band changes its position only slightly in the respective complexes, but the appearance of a new band at considerably lower wavenumber indicates the coordination of only one of the azomethine nitrogen atoms to molybdenum. The presence of several medium intensity bands between 2800 and 2500 cm^{-1} in the ligands as well as in the complexes suggests the existence of C-H stretching due to -CH_2. The coordination of pyridine is characterized by the appearance of the ring breathing mode, the totally symmetric ring stretching mode, the in-plane antisymmetric ring stretching mode and the in-plane totally symmetric ring breathing mode at ca. 1000, 1600, 1440 and 1040 cm^{-1}, respectively [51]. In addition, these complexes display two sharp bands at 914-928 and 889-903 cm^{-1} due to the ν_{asym}(O=Mo=O) and ν_{sym}(O=Mo=O) modes, respectively. These data indicate the presence of a cis-[$Mo^{VI}O_2$] structure [48].

<<Table 4>>

3.5. Electronic spectral studies

Table 5 includes the electronic spectral data of the ligands and the complexes. The electronic spectra of H_3sal-dahp (**I**), H_3clsal-dahp (**II**) and H_3brsal-dahp (**III**) exhibit four UV absorption bands. Based on their extinction coefficients, these bands are interpreted as n→π* (317-329 nm), π→π* (254-256 and 277-279 nm) and φ →φ* (217-225 nm) transitions. The additional band for the π→π* transition is possibly due to splitting of this transition. In the complexes, the two π→π* bands collapse into one band and appear at an average value (259-264 nm) while the n→π* band appears at nearly the same position. In addition, all the complexes exhibit a medium intensity band at 413-431 nm due to a ligand to metal charge transfer (LMCT)

transition from the phenolate oxygen atom to an empty d-orbital of the molybdenum. As Mo^{VI}-complexes have a $4d^0$ configuration, a d→d band is not expected.

<<Table 5>>

3.6. ^1H and ^{13}C NMR studies

The coordinating modes of H_3sal-dahp (**I**), H_3clsal-dahp (**II**) and H_3brsal-dahp (**III**) were also confirmed by comparing their ^1H NMR spectral patterns with those of the corresponding complexes. The relevant spectral data are collected in Table 6. Fig. 5 reproduces the ^1H NMR spectra of a representative ligand and its complexes. All the ligands show two signals at δ = 13.56 (br, 2H) and 5.24 (br, 1H) ppm due to the phenolic and alcoholic OH, respectively. The absence of a signal due to the alcoholic OH in the complexes is in conformity with the coordination of the alcoholic oxygen to the molybdenum, while the existence of a phenolic signal integrating to one proton indicates the involvement of one of the phenolic oxygens in coordination after proton replacement. Similarly, the appearance of two signals due to azomethine protons (each equivalent to 1H) with coordination-induced shifts [$\Delta\delta$ = [δ(complex) – δ(free ligand)] of 0.25 ppm in the complexes demonstrates the coordination of only one of the azomethine groups to molybdenum. Appearance of two signals of equal intensity for azomethine groups rules out the possibility of a dynamic equilibrium between the free and coordinated nitrogen functions in solution. The –CH proton is also affected and appears at $\Delta\delta$ = 0.62 ppm downfield compared to the free ligands. Similarly, the $–CH_2$ group that forms a five membered ring upon coordination of the alcoholic oxygen atom to the molybdenum also shows a significant downfield shift. Signals due to aromatic protons and the other CH_2 group appear in the expected regions in the spectra of the ligands as well as the complexes, with slight shifts in their positions.

<<Table 6>>

The ^{13}C NMR spectra of the ligands and the complexes also provide useful information for the elucidation of the structures of the complexes. Spectra of the representative ligand H_3sal-dahp (**1**) and its complexes **1** and **4** are presented in Fig. 6, while Table 7 provides the entire

spectral data. Assignments of the peaks are based on the intensity patterns, the chemical shift and on the coordination-induced shifts ($\Delta\delta$) of the signals for carbon atoms in the vicinity of coordinating atoms [52]. All the ligands display 9 signals corresponding to 17 carbon atoms due to the presence of a centre of symmetry. As expected, 17 signals were observed for complexes **1**-**3** and 20 for the pyridine analogues due to the asymmetry generated after coordination of the ligands to molybdenum. A large coordination-induced shift of the signal for the carbon atom bearing the alcoholic oxygen (C9) atom demonstrates coordination of the alcoholic oxygen to the molybdenum. All the ligands display a single signal each for the azomethine (C1 and C11) and the phenolate carbon atoms. The appearance of two distinct signals each due to the azomethine (C1 and C11) and the phenolate carbons (C3 and C13) against a single signal each for these carbons in the ligands suggest the involvement of only one set of the azomethine nitrogen and the phenolate oxygen atoms in coordination. Again these signals suggest no possibility of a dynamic equilibrium between the coordinated and free functional groups. Three distinct signals appear in the δ = 134.7-150.0 ppm region in complexes **4**-**6** due to the coordinated pyridine. A considerable separation ($\delta_{C8} - \delta_{C10}$ = 2.1 - 2.4 ppm) in the signals due to methylene carbons (C8 and C10) has also been noticed due to the involvement of C8 in ring formation. Thus, the ^{1}H and ^{13}C NMR data confirm the IR and UV/Vis evidence.

<<Figures 5 and 6>> <<Table 7>>

3.7. Reactivity of dioxidomolybdenum(VI) complexes with H_2O_2

It is known that dioxidomolybdenum(VI) complexes react with H_2O_2 to give the corresponding $[Mo^{VI}O(O_2)]^{2+}$ complexes. To support the reaction mechanism, we tried to isolate such peroxido complexes in the solid state, but failed due to the insolubility of the corresponding dioxido complexes in methanol/ethanol along with difficulty in isolating peroxidomolybdenum(VI) complexes from a solvent like DMSO. However, the generation of such species has been established in DMSO by electronic absorption spectroscopy. In a typical reaction, 15 mL of ca. 10^{-3} M solution of $[MoO_2(Hclsal\text{-}dahp)(H_2O)]$ (**2**) was treated with one drop portion of 30% aqueous H_2O_2 (0.253 g, 2.3 mmol) dissolved in 5 mL of DMSO and the

resultant spectroscopic changes are presented in Fig. 7 (b). The weak and broad charge transfer band appearing at 415 nm slowly increases in intensity along with broadening and shifting to 425 nm. A similar titration with a dilute solution of the complex causes a small shift of the 328 nm band to 333 nm along with onlya marginal change in intensity, while the 264 nm band increases its intensity considerably and finally disappears; Fig. 7(a). These changes indicate the interaction of $[MoO_2(Hclsal\text{-}dahp)(H_2O)]$ (**2**) with H_2O_2 and the plausible formation of $[Mo^{VI}O(O_2)(Hclsal\text{-}dahp)]$ in DMSO (Eq. 3). Similar changes have also been noted for other complexes; Figs. 7(c) and 7(d) (only the 380-500 nm region is shown).

<<Figure 7>>

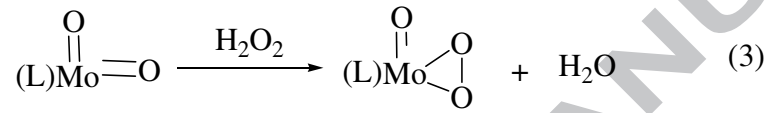

(3)

(L = ligand)

3.8. Catalytic activity studies

3.8.1. Oxidative bromination of styrene

The oxidative bromination of styrene using **1**, **2** and **3** as catalyst precursors in the presence of KBr, 70% aqueous $HClO_4$ and 30 % aqueous H_2O_2 under a bi-phasic (CH_2Cl_2-H_2O) system gave mainly three major products, namely, 1,2-dibromo-1-phenylethane, 2-bromo-1-phenylethane-1-ol and 1-phenylethane-1,2-diol (Scheme 3), along with some minor products like benzaldehyde, styrene epoxide, benzoic acid and 4-bromostyrene whose overall percentage is extremely low compared to the total of the main products. The obtained main products were confirmed by ^1H NMR spectroscopy as well as by GC–MS after their separation, and are the same as reported using vanadium complexes as catalysts [53-55].

<<Scheme 3>>

The reaction conditions were optimized for: i) the maximum oxidative bromination of styrene, irrespective of the selectivity of products and ii) for the maximum formation of 2-bromo-1-phenylethane-1-ol, considering different parameters like amounts of catalyst, H_2O_2,

KBr and $HClO_4$, using $[Mo^{VI}O_2(Hsal\text{-}dahp)(H_2O)]$ (**1**) as a representative catalyst precursor. Thus, for 10 mmol of styrene (1.04 g), three different amounts of catalyst (0.001, 0.0015 and 0.002 g), 30 % aqueous H_2O_2 (10, 20 and 30 mmol), KBr (20, 30 and 40 mmol) and $HClO_4$ (20, 30 and 40 mmol, added in four equal portions to the reaction mixture, first portion at t = 0 and other three portions after 15 minute intervals) were taken in a dichloromethane-water (40 mL, v/v) mixture and the reaction was carried out at room temperature. Acid (here $HClO_4$) was found to be essential to carry out the catalytic bromination. Its way of addition to the reaction mixture controls the stability of the substrate, while its amount has great influence on the conversion and selectivity of the products. The complexes slowly decompose during the reaction; decomposition is slowed down, if $HClO_4$ is successively added in four portions during the 1 h reaction time.

Table 8 summarizes all the conditions considered and the corresponding percentage of oxidative bromination of styrene along with the selectivity of different reaction products. It is clear from the data presented in the table that the conversions are competitive, 97-99%, under most reaction conditions. However, the selectivity of the products differs on varying the reagents. The best suited conditions (entry no. 9 of Table 8) for the maximum oxidative bromination of styrene, with 98% conversion are: catalyst (0.001g), 30 % aqueous H_2O_2 (2.27 g, 20 mmol), KBr (2.38 g, 20 mmol) and $HClO_4$ (4.29 g, 30 mmol) in dichloromethane-water (40 mL, v/v) mixture). Under these conditions the selectivity of different major products follows the order: phenylethane-1,2-diol (67%) > 1,2-dibromo-1-phenylethane (21%) > 2-bromo-1-phenylethane-1-ol (3%). Using 0.001 g of catalyst and considering the substrate to different reagents in the molar ratio of 1:2 (entry no 8 of Table 8) gave the highest selectivity of 2-bromo-1-phenylethane-1-ol (34%) with no formation of 1,2-dibromo-1-phenylethane amongst all the conditions applied. Increasing the amounts of KBr as well as acid results in the increased formation of the dibromo product at the expense of the monobromo one, while increasing the oxidant improves the formation of mainly phenylethane-1,2-diol. Under the optimized conditions for the maximum conversion of styrene, the other catalysts, i.e. **2** and **3**, exhibit similar catalytic activity, along with similar selectivity of different products (entries no 10 and 11, and Fig. 8).

Negative controls under the conditions presented in entries no. 12 and 13 of Table 8 resulted in 44 and 60 % conversion respectively, and formation of only two products was observed.

<<Table 8>> <<Figure 8>>

The oxidative bromination of styrene and the selectivity of different reaction products for catalysts **1**, **2** and **3** under the optimized reaction conditions (see entries no. 9, 10 and 11 of Table 8) have also been analyzed as a function of time and are presented in Fig. 9 (b, c and d). The formation of all three products starts with the conversion of styrene and follows very similar patterns with the elapse of time. Thus the selectivity of 46-55 % of 1-phenylethane-1,2-diol at t = 15 min improves with time and reaches 63-72 % at the end of 1 h while that of 2-bromo-1-phenylethane-1-ol (bromohydrin) starts at 42-50 % at t = 15 min and goes down to 1-3% at the end of the reaction. The formation of 1,2-dibromo-1-phenylethane is nearly zero at the beginning but slowly improves with time and reaches 15-27%. It seems that the formation of 1-phenylethane-1,2-diol occurs at the expense of the mono bromo derivative (see Scheme 4). Under the conditions presented in entry no. 8, the selectivity of the formation of the two products at t = 15 min follows the order: 2-bromo-1-phenylethane-1-ol (61%) > 1-phenylethane-1,2-diol (33%) but it reverses and follows the order: 1-phenylethane-1,2-diol 61% > 2-bromo-1-phenylethane-1-ol (34%) at the end of 1 h (Fig. 9 (a)).

<<Figure 9>>

As observed in vanadium complexes [40-42], catalytically generated HOBr, by the reaction of molybdenum complexes with KBr in the presence of H_2O_2 and $HClO_4$, reacts with styrene to give the bromonium ion as an intermediate. The nucleophile Br^- as well as H_2O both may attack the α-carbon of the intermediate to give 1,2-dibromo-1-phenylethane and 2-bromo-1-phenylethane-1-ol, respectively (Scheme 4). The formation of the dibromo product, in most cases at later stage, is possibly due to the presence of a lower amount of the brominating reagent generated initially. The nucleophile H_2O may further attack the α-carbon of 2-bromo-1-phenylethane-1-ol to give 1-phenylethane-1,2-diol. All these justify the formation of 1-phenylethane-1,2-diol in the highest yield. Oxidative bromination of styrene has mainly been

reported by vanadium complexes. However, the catalytic potential shown by molybdenum complexes for the oxidative bromination of styrene reported here compares well with those shown by vanadium complexes [55].

<<Scheme 4>>

3.8.2. Oxidation of methyl phenyl sulfide

The sulfur atom of the organic sulfide is electron rich and undergoes electrophilic oxidation, catalyzed by several molybdenum oxotransferases [56,57]. Chakravarthy et al. have proposed a possible mechanism for the catalytic sulfoxidation of methyl phenyl sulfide [38]. Such an oxidation of methyl phenyl sulfide was tested using complexes **1**, **2** and **3** as catalysts and the corresponding sulfoxide, as well as the sulfone, was obtained as shown in Scheme 5. Sulfoxides and sulfones, the oxidation product of sulfides, are useful precursors for biologically and chemically important compounds [58,59]. Sulfoxides have been used as ligands in asymmetric catalysis [60] and as oxotransfer reagents [61] and sulfones have been employed for stabilizing radicals [62] and anions, [63] and acting as cationic synthons [64].

<<Scheme 5>>

Again, [$Mo^{VI}O_2$(Hsal-dahp)(H_2O)] (**1**) was taken as a representative catalyst and various parameters were optimized to get the maximum oxidation of methyl phenyl sulfide. Thus for 10 mmol (1.24 g) of methyl phenyl sulfide, the amount of catalyst (0.001 g, 0.00015 g and 0.002 g), 30% aqueous H_2O_2 (10, 20 and 30 mmol) and volume of acetonitrile (5, 10 and 15 mL) were varied and the reaction was carried out at room temperature. The conversions obtained with all these conditions, plotted as a function of time, are presented in Fig. 10 (a, b and c). Table S1 (see supporting information) summarizes all the conditions and conversions obtained under a particular set of conditions. The optimized conditions for highest catalytic activity, with 98% conversion of methyl phenyl sulfide, were concluded as: methyl phenyl sulfide (1.24 g, 10 mmol), catalyst **1** (0.0015 g), 30% aqueous H_2O_2 (2.27 g, 20 mmol) and CH_3CN (5 mL).

The percent conversion of methyl phenyl sulfide under the optimised reaction conditions and the selectivity of the reaction products as a function of time are shown in Fig. 10(d). It is clear from the plot that both the products start to form with the conversion of methyl phenyl

sulfide. However, the initial selectivity of 76 % for methyl phenyl sulfoxide at 38 % conversion of methyl phenyl sulfide in the first half an hour starts to decrease and reaches 66.8 % after 2 h of reaction time. Thus, the initially formed sulfoxide partly reacts with H_2O_2 present in the reaction mixture to give the sulfone.

<<Figure 10>>

The other catalysts [MoO_2(Hclsal-dahp)(H_2O)] (**2**) and [MoO_2(Hbrsal-dahp)(H_2O)] (**3**), tested under the above optimized reaction conditions, gave maxima of 97 and 96% conversion, respectively, Fig. S2. Thus, amongst the three complexes, the catalytic efficiency varies in the order: (**1**) > (**2**) > (**3**). The selectivity of different products along with the conversion and turnover frequency for these catalysts are presented in Table 9. It is clear from the data presented in the table that the selectivity for the formation of methyl phenyl sulfoxide is nearly the same in all three cases, and it is always higher than that for methyl phenyl sulfone.

<<Table 9>>

The catalytic potential of these complexes in the oxidation of methyl phenyl sulfide are either better than or compare well with those reported using *cis*-[$Mo^{VI}O_2$]-(ONO) complexes, where ONO stands for simple as well as chiral Schiff base ligands [38,39].

3.8.3. Oxidation of benzoin

The oxidation of benzoin has attracted the attention of researchers because one of its oxidized products, benzil, is a very useful intermediate for the synthesis of heterocyclic compounds and benzylic acid rearrangements [65]. The oxidation of benzoin, catalyzed by Mo^{VI}-O_2 complexes was carried out in refluxing methanol and the products mainly obtained were benzoic acid, benzaldehyde-dimethylacetal, methylbenzoate and benzil; Scheme 6.

<<Scheme 6>>

The reaction conditions were optimized using 5 mmol (1.06 g) of benzoin, varying the amount of catalyst (0.0005, 0.001 and 0.0015 g), 30 % aqueous H_2O_2 (10, 15 and 20 mmol) and

volume of methanol (10, 15 and 20 mL). About 4 h was required to attain the equilibrium. Figs. S3-S6 of the supporting information and Table 10 summarize all the conditions and conversions obtained under a particular set of conditions. From these experiments the best suited reaction conditions concluded for the maximum oxidation of benzoin are: [MoO_2(Hsal-dahp)(H_2O)] (0.0005 g), benzoin (1.06 g, 5 mmol), 30% aqueous H_2O_2 (1.7 g, 15 mmol) and refluxing methanol (10 mL). Fig. 11 presents the selectivity of the products along with the conversion of benzoin as a function of time under these conditions. It is clear from the plot that all the products form with the conversion of benzoin. The highest selectivity of benzoic acid (*ca*. 54%) was observed in the first hour. With the elapse of time its selectivity slowly decreased and finally becomes almost constant and reaches 40 % after 4 h. Similarly benzil starts with ca. 21% and reaches 15 %. The selectivity of benzaldehyde-dimethylacetal and methyl benzoate increases continuously from 4 to 13 % and 21 to 32 %, respectively in 4 h. Thus, with the maximum benzoin oxidation of 95 % after 4 h of reaction time, the selectivity of the reaction products varies in the order: benzoic acid (40%) > methyl benzoate (32%), > benzil (15%) > benzaldehyde-dimethylacetal (13%).

<<Figure 11>> <<Table 10>>

Under the above reaction conditions, the catalytic activity of the other complexes for the oxidation of benzoin were also tested and details of the conversion of benzoin, turnover frequency and selectivity of the various products obtained after 4 h of reaction are summarized in Table 11. As shown, all the complexes show equally good catalytic activity, with ca. 95% conversion of benzoin, and the substituent on the benzene ring has no influence on their activity. Similarly, the selectivity of different products, though slightly differing for different complexes, essentially follows the same order for all the complexes. The catalytic potential of these complexes for the oxidation of benzoin are much better than the one obtained by the polymer anchored [$Mo^{VI}O_2$(salphen)] catalyst, but the later one is more selective to benzil [31].

<<Table 11>>

4. Conclusions

Dioxidomolybdenum(VI) complexes with dibasic tridentate ligands are mostly known to exist either as five coordinated monomeric $[Mo^{VI}O_2L]$ [43], five coordinated oligimeric $[Mo^{VI}O_2L]^n$ (with a [Mo=O→Mo] [48] structure) or six coordinated $[Mo^{VI}O_2L(D)]$ [48] (D = coordinating solvent which is normally used to prepare the complex) complexes. The complexes reported here belongs to the latter category, where the ligands only behave as a dibasic tridentate ONO donor and other functional groups are free from coordination. However, in-situ generated H_3clsal-dahp in methanolic solution, on reaction with $[Mo^{VI}O_2(acac)_2]$ in DMSO, gave $[Mo^{VI}O_2$(clsal-hdap)(DMSO)$]_4[Mo_8O_{26}]\cdot$6DMSO (**7**) where the non-coordinated azomethine nitrogen hydrolyzes giving a free protonated amine group; the $[Mo_8O_{26}]^{4-}$ anion is stabilized through hydrogen bonding with the $[Mo^{VI}O_2$(clsal-hdap)(DMSO)$]^+$ cation. The dioxidomolybdenum(VI) complexes $[Mo^{VI}O_2$(Hsal-dahp)$(H_2O)]$ (**1**), $[Mo^{VI}O_2$(Hclsal-dahp)$(H_2O)]$ (**2**) and $[Mo^{VI}O_2$(Hbrsal-dahp)$(H_2O)]$ (**3**) present good functional models of haloperoxidases in that they catalyze the oxidative bromination of styrene, giving 1,2-dibromo-1-phenyl-ethane, 1-phenylethane-1,2-diol and 2-bromo-1-phenylethane-1-ol. These complexes are also good catalyst precursors for the oxidation of methyl phenyl sulfide, an activity shown by molybdenum oxotransferases, and benzoin.

Appendix A. Supplementary material

CCDC 935233 for **7** and 935234 for **3a** contain the supplementary crystallographic data for the structures reported in this paper. These data can be obtained free of charge via http://www.ccdc.cam.ac.uk/conts/retrieving.html, or from the Cambridge Crystallographic Data Centre, 12 Union Road, Cambridge CB2 1EZ, UK; fax: (+44) 1223 336 033; or e-mail: deposit@ccdc.cam.ac.uk. Supplementary data associated with this article can be found in the online version.

Acknowledgments

M. R. M. thanks the Department of Science and Technology (DST), Government of India, New Delhi (SR/S1/IC-32/2010) for financial support in procuring gas chromatograph. SD acknowledges the University Grant Commission, New Delhi for a Junior Research fellowship.

References

[1] E.I. Stiefel, Science 272 (1996) 1599-1600.

[2] M.M. Abu-omar, A. Loaiza, N. Hontzeas, Chem. Rev. 105 (2005) 2227-2252.

[3] C. A. McAuliffe, F. P. Mc Cullough, M. J. Parrott, C. A. Rice, B. J. Sayle, W. Levanson, J. Chem. Soc., Dalton Trans. (1977) 1762-1766.

[4] R.H. Holm, Coord. Chem. Rev. 100 (1990) 183-221.

[5] J.T. Spence, Coord. Chem. Rev. 48 (1983) 59-82.

[6] A. Thapper, A. Behrens, J. Fryxelius, M. H. Johansson, F. Prestopino, M. Czaun, D. Rehder, E. Nordlander, Dalton Trans. 21 (2005) 3566-3571.

[7] R. Hahn, W. A. Herrmann, G. R. J. Artens, M. Kleine, Polyhedron 14 (1995) 2953-2960.

[8] J. Liimatainen, A. Lehtonen, R. Sillanpaa, Polyhedron 19 (2000) 1133-1138.

[9] U. Sandbhor, S. Padhye, E. Sinn. Transition Met. Chem. 27 (2002) 681-685.

[10] M. Cindric, N. Strukan, V. Vrdoljak, B. Kamenar, *Z.* Anorg. Allg. Chemie 628 (2002) 2113-2117.

[11] H. Arzoumanian, G. Agrifoglio, H. Krentzien, M. Capparelli, J. Chem. Soc., Chem. Commun. (1995), 655-656.

[12] H. Arzoumanian, L. Maurino, G. Agrifoglio, J. Mol. Catal. A: Chem. 117 (1997) 471-478.

[13] M.M. Farahani, F. Farzaneh, M. Ghandi, Catal. Commun. 8 (2007) 6-10.

[14] M.M. Farahani, F. Farzaneh, M. Ghandi, J. Mol. Catal. A: Chem. 248 (2006) 53-60.

[15] K. Ambroziak, R. Pelech, E. Milchert, T. Dziembowska, Z. Rozwadowski, J. Mol. Catal. A: Chem. 211 (2004) 9-16.

[16] Y. Sui, X. Zeng, X. Fang, X. Fu, Y. Xiao, L. Chen, M. Li, S. J. Cheng, Mol. Catal. A: Chem. 270 (2007) 61-67.

[17] J. Zhao, X. Zhou, A.M. Santos, E. Herdtweck, C. C. Romao, F.E. Kühn, Dalton Trans. (2003) 3736-3742.

[18] X. Zhou, J. Zhao, A.M. Santos, F.E. Kühn, Naturforsch. 59b (2004) 1223-1228.

[19] J. M. Sobczak, J. J. Zi lkowski, Appl. Catal. A 248 (2003) 261-268.

[20] M. Bagherzadeh, R. Latifi, L. Tahsini, V. Amani, A. Ellern, L. K. Woo, Polyhedron 28 (2009) 2517-2521.

[21] A. Rezaeifard, I. Sheikhshoaie, N. Monadi, M. Alipour, Polyhedron 29 (2010) 2703-2709.

[22] J. Pisk, D. Agustin, V. Vrdoljak, R. Poli, Adv. Synth. Catal. 353 (2011) 2910-2914.

[23] J. Pisk, B. Prugovečki, D. Matković-Čalogović, R. Poli, D. Agustin, V. Vrdoljak, Polyhedron 33 (2012) 441-449.

[24] K.C. Gupta, A.K. Sutar, Coord. Chem. Rev. 252 (2008) 1420-1450.

[25] M. E. Judmaier, C. Holzer, M. Volpe, N. C. Mösch-Zanetti, Inorg. Chem. 51 (2012) 9956-9966.

[26] X. Lei, N. Chelamalla, Polyhedron, 49, (2013) 244-251.

[27] M.R. Maurya, Curr. Org. Chem. 16 (2012) 73-88.

[28] K. I. Smith, L. L. Borer, M. M. Olmstead, Inorg. Chem. 42 (2003) 7410-7415.

[29] M. R. Maurya, M. Bisht, N. Chaudhary, F. Avecilla, U. Kumar, H.-F. Hsu, Polyhedron 54 (2013) 180-188.

[30] K. Jeyakumar, D.K. Chand, J. Chem. Sci. 123 (2011) 187-199.

[31] R.K. Bhatia, G.N. Rao, J. Mol. Catal. A: Chem. 121 (1997) 171-178.

[32] M.R. Maurya, U. Kumar, P. Manikandan, Dalton Trans. (2006) 3561-3575.

[33] M. R. Maurya, A. Arya, P. Adão, J. Costa Pessoa, Appl. Catal. A: Gen. 351 (2008) 239-252.

[34] K. Jeyakumar, D.K. Chand, J. Chem. Sci. 121 (2009) 111-123.

[35] Z. Hu, X. Fu, Y. Li, Inorg. Chem. Commun. 14 (2011) 497-501.

[36] M. Bagherzadeh, M. M. Haghdoost, M. Amini, P.G. Derakhshandeh, Catal. Commun. 23 (2012) 14-19

[37] K. Jeyakumar, D.K. Chand, J. Chem. Sci. 121 (2009) 111-123.

[38] R. D. Chakravarthy, K. Suresh, V. Ramkumar, D. K. Chand, Inorg. Chim. Acta 376 (2011) 57-63.

[39] I. Sheikhshoaie, A. Rezaeifard, N. Monadi, S. Kaafi, Polyhedron 28 (2009) 733-738.

[40] A. Butler, M. J. Clague, G. E. Meister, Chem. Rev. 94 (1994) 625-638.

[41] C. J. Schneider, J. E. Penner-Hahn, V. L. Pecoraro, J. Am. Chem. Soc. 130 (2008) 2712-2713.

[42] P. Adao, J. Costa Pessoa, R. T. Henriques, M. L. Kuznetsov, F. Avecilla, M. R. Maurya, U. Kumar, I. Correia, Inorg. Chem. 48 (2009) 3542-3561.

[43] J.J. Boruah, S.P. Das, R. Borah, S.R. Gogoi, N.S. Islam, Polyhedron, 52 (2013) 246-254.

[44] G. J.J. Chen, J. W. McDonald, W. E. Newton, Inorg. Chem. 15 (1976) 2612-2615.

[45] M. R. Maurya, M. Bisht, F. Avecilla, Indian J. Chem. 50A (2011) 1562-1573.

[46] G. M. Sheldrick, *SHELXS-97:* An Integrated System for Solving Crystal Structures from Diffraction Data, Revision 5.1, University of Göttingen, Germany, (1997).

[47] a) R. Dinda, P. Sengupta, S. Ghosh, W. S. Sheldrick, Eur. J. Inorg. Chem. (2003), 363-369; b) T. A. Hanna, A. K. Ghosh, C. Ibarra, M. A. Mendez-Rojas, A. L. Rheingold, W. H. Watson, Inorg. Chem. 43 (2004) 1511-1516.

[48] A. Syamal, M.R. Maurya, Coord. Chem. Rev. 95 (1989) 183-238.

[49] a) A. J. Bridgeman, G. Cavigliasso, Inorg. Chem. 41 (2002) 3500-3507; b) C.J. Carrasco, F. Montilla, E. Álvarez, M. Herbert, A. Galindo, Polyhedron 54, (2013) 123-130.

[50] K. H. Tytko, J. Mehmke, S. Fischer, Struct. Bonding (Berlin) 93 (1999) 129-321.

[51] M.R. Maurya, D.C. Antony, S. Gopinathan, C. Gopinathan, Polyhedron 12 (1993) 2731-2736.

[52] A. D. Keramidas, A. B. Papaioannou, A. Vlahos, T. A. Kabanos, G. Bonas, A. Makriyannis, C. P. Rapropoulou, A. Terzis, Inorg. Chem. 35 (1996) 357-367.

[53] V. Conte, B. Floris, Inorg. Chim. Acta 363 (2010) 1935-1946.

[54] V. Conte, A. Coletti, B. Floris, G. Licini, C. Zonta, Coord. Chem. Rev. 255 (2011) 2165-2177.

[55] (a) M.R. Maurya, C. Haldar, A. A. Khan, A. Salahuddin, A. Azam, A. Kumar, J. Costa Pessoa, Eur. J. Inorg. Chem. (2012), 2560-2577; (b) M.R. Maurya, C. Haldar, A. Kumar M.L. Kuznetsov, F. Avecilla, J. Costa Pessoa, Dalton Trans. DOI: 10.1039/c3dt50469g, 2013.

[56] M.A. Anderson, A. Willets, S. Allenmark, J. Org. Chem. 62 (1997) 8455-8458.

[57] H. B. ten Brink, H. E. Schoemaker, R. Wever, Eur. J. Biochem. 268 (2001) 132-138.

[58] E. Clark, in: Encyclopedia of Chemical Technology, (Eds.: J.I. Kroschwitz, M. Howe-Grant), 4th ed., Wiley, New York, (1997), vol. 23, pp. 134-146.

[59] P.C.B. Page, Organosulfur Chemistry I and II, Springer, Berlin, (1999).

[60] I. Fernandez, N. Khiar, Chem. Rev. 103 (2003) 3651-3705.

[61] A.M. Khenkin, R. Neumann, J. Am. Chem. Soc. 124 (2002) 4198-4199.

[62] L.A. Paquette, Synlett. 1 (2001) 1-12.

[63] C. Najera, J.M. Sansano, Recent Res. Dev. Org. Chem. 2 (1998) 637-683.

[64] R. Chinchila, C. Najera, Recent Res. Dev. Org. Chem. 1 (1997) 437-467.

[65] G. B. Gill, in: Comprehensive Organic Synthesis, (Ed.: G. Pattenden), Pergamon Press, New York, (1991), vol. 3, p. 821-838.

Schemes

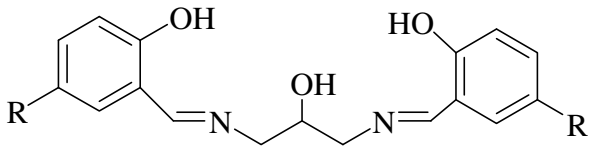

R = H: H_3sal-dahp (**I**)

R = Cl: H_3clsal-dahp (**II**)

R = Br: H_3brsal-dahp (**III**)

Scheme 1. Structure of the ligands designated by **I**, **II** and **III** used in this work.

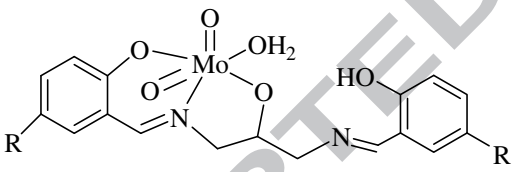

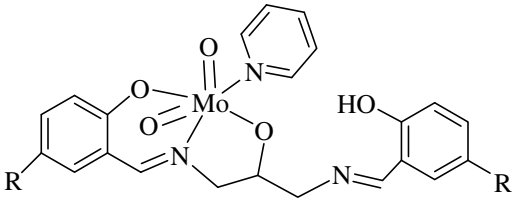

R = H: [$Mo^{VI}O_2$(Hsal-dahp)(H_2O)] (**1**)
R = Cl: [$Mo^{VI}O_2$(Hclsal-dahp)(H_2O)] (**2**)
R = Br: [$Mo^{VI}O_2$(Hbrsal-dahp)(H_2O)] (**3**)

R = H: [$Mo^{VI}O_2$(Hsal-dahp)(py)] (**4**)
R = Cl: [$Mo^{VI}O_2$(Hclsal-dahp)(py)] (**5**)
R = Br: [$Mo^{VI}O_2$(Hbrsal-dahp)(py)] (**6**)

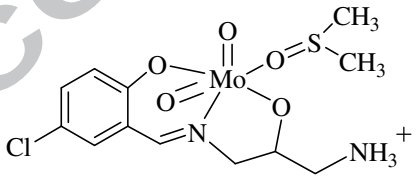

[$Mo^{VI}O_2$(Hclsal-hdap)(DMSO)]$^+$ (Cation part of **7**)

Scheme 2. Proposed structure of the complexes reported in this contribution.

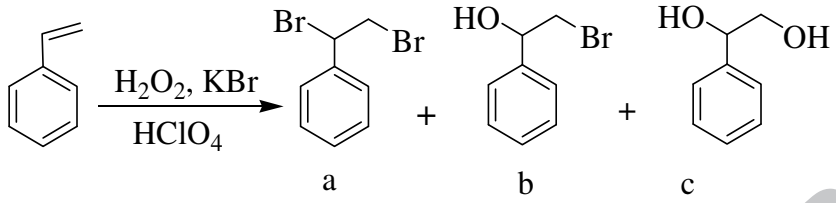

Scheme 3. Main products obtained by oxidative bromination of styrene: (a) 1,2-dibromo-1-phenylethane (dibromide), (b) 2-bromo-1-phenylethane-1-ol (a bromohydrin) and (c) 1-phenylethane-1,2-diol.

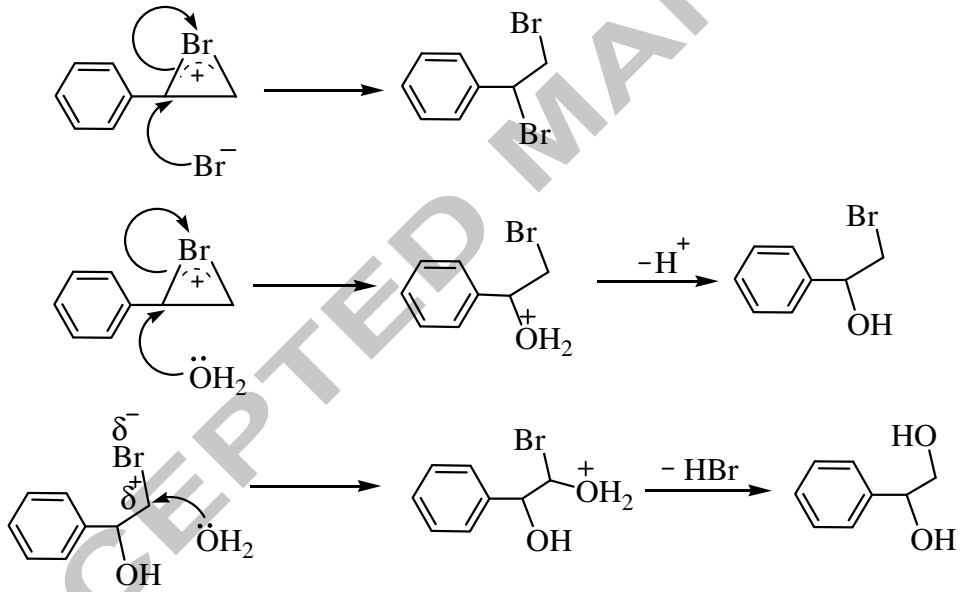

Scheme 4. Mechanism of action of HOBr on styrene.

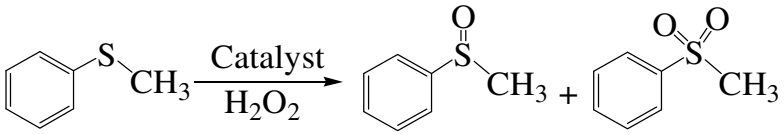

Scheme 5. Oxidation products of methyl phenyl sulfide with H_2O_2.

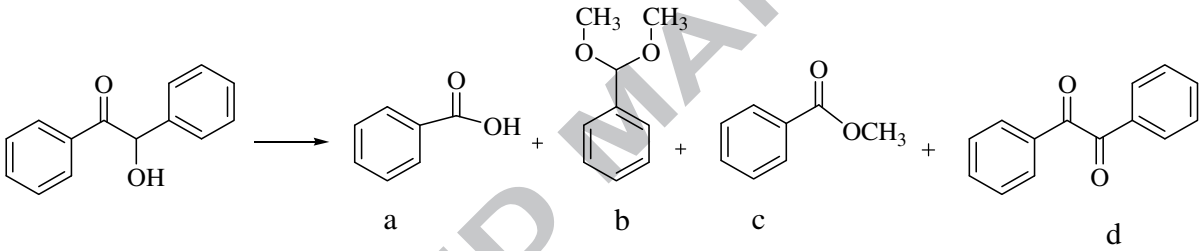

Scheme 6. Various oxidation products of benzoin: (a) benzoic acid, (b) benzaldehyde-dimethylacetal, (c) methylbenzoate and (d) benzil.

Figures

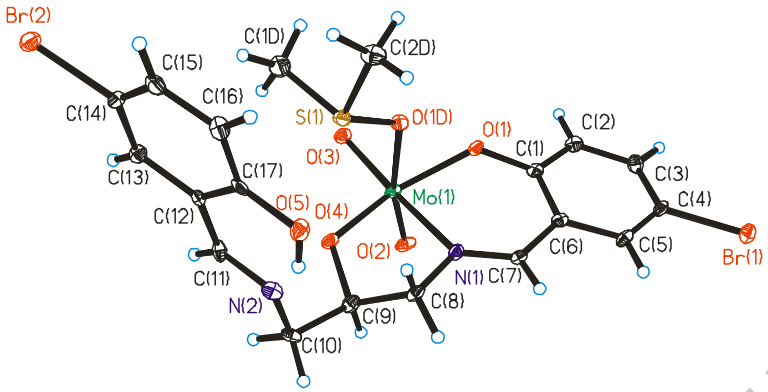

Fig. 1. ORTEP plot of the complex [Mo^{VI}O$_2$(Hbrsal-dahp)(DMSO)] (**3a**). All the non-hydrogen atoms are presented by their 30% probability ellipsoids.

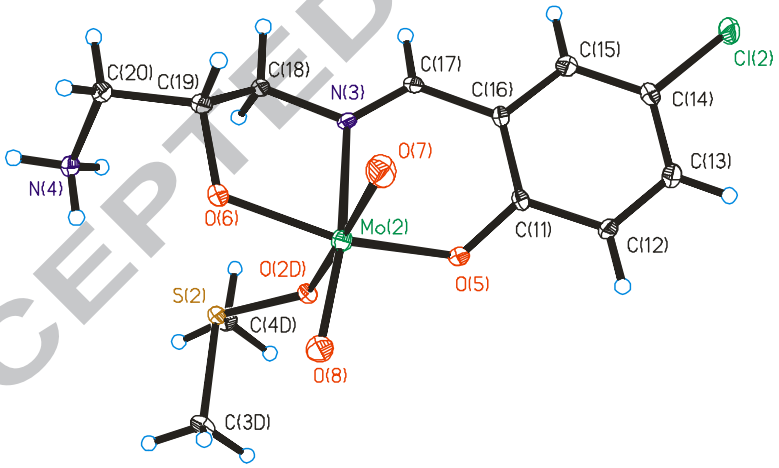

Fig. 2. ORTEP plot of cation [Mo^{VI}O$_2$(Hclsal-hdap)(DMSO)]$^+$ in the compound [Mo^{VI}O$_2$(Hclsal-hdap)(DMSO)]$_4$[Mo$_8$O$_{26}$]·6DMSO (**7**). All the non-hydrogen atoms are presented by their 30% probability ellipsoids.

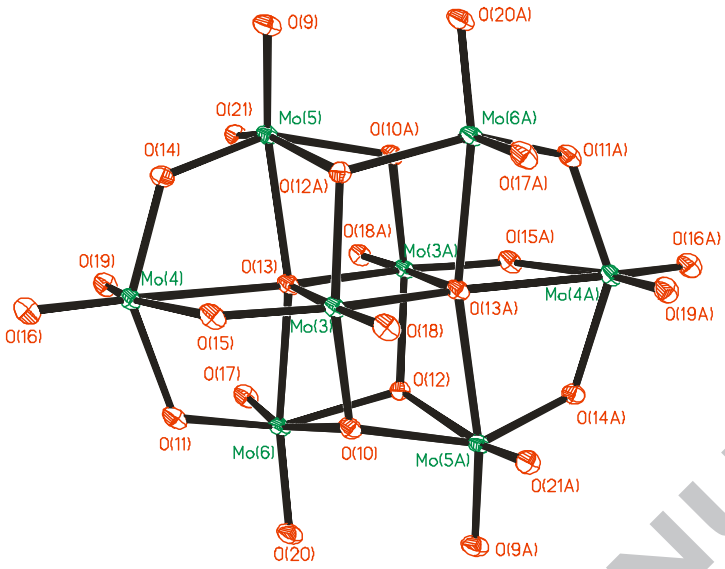

Fig. 3. Structural and atom labelling scheme for the β-$[Mo_8O_{26}]^{4-}$ anion in the compound $[Mo^{VI}O_2(Hclsal\text{-}hdap)(DMSO)]_4[Mo_8O_{26}]\cdot 6DMSO$ (**7**).

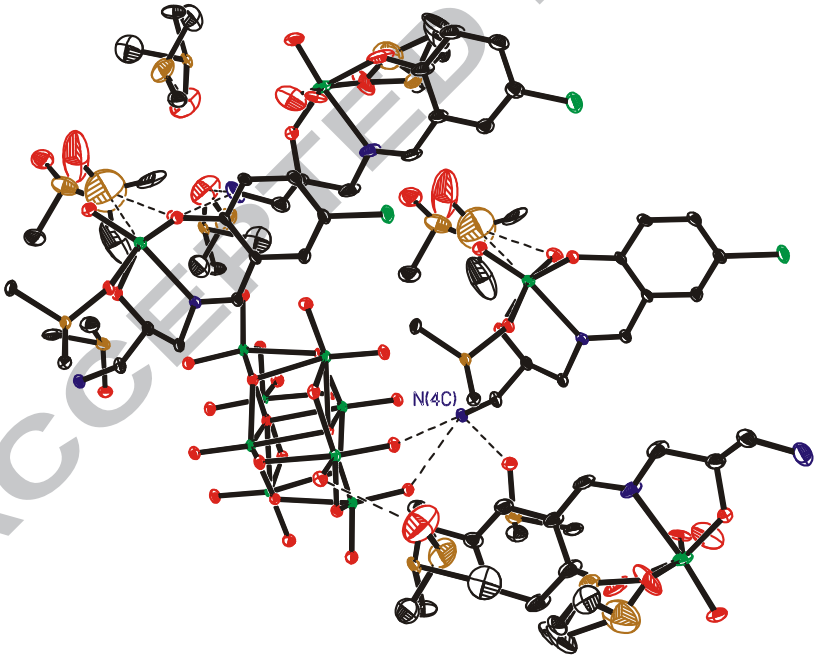

Fig. 4. Crystal packing of $[Mo^{VI}O_2(Hclsal\text{-}hdap)(DMSO)]_4[Mo_8O_{26}]\cdot 6DMSO$ (**7**) along with the hydrogen bonding scheme.

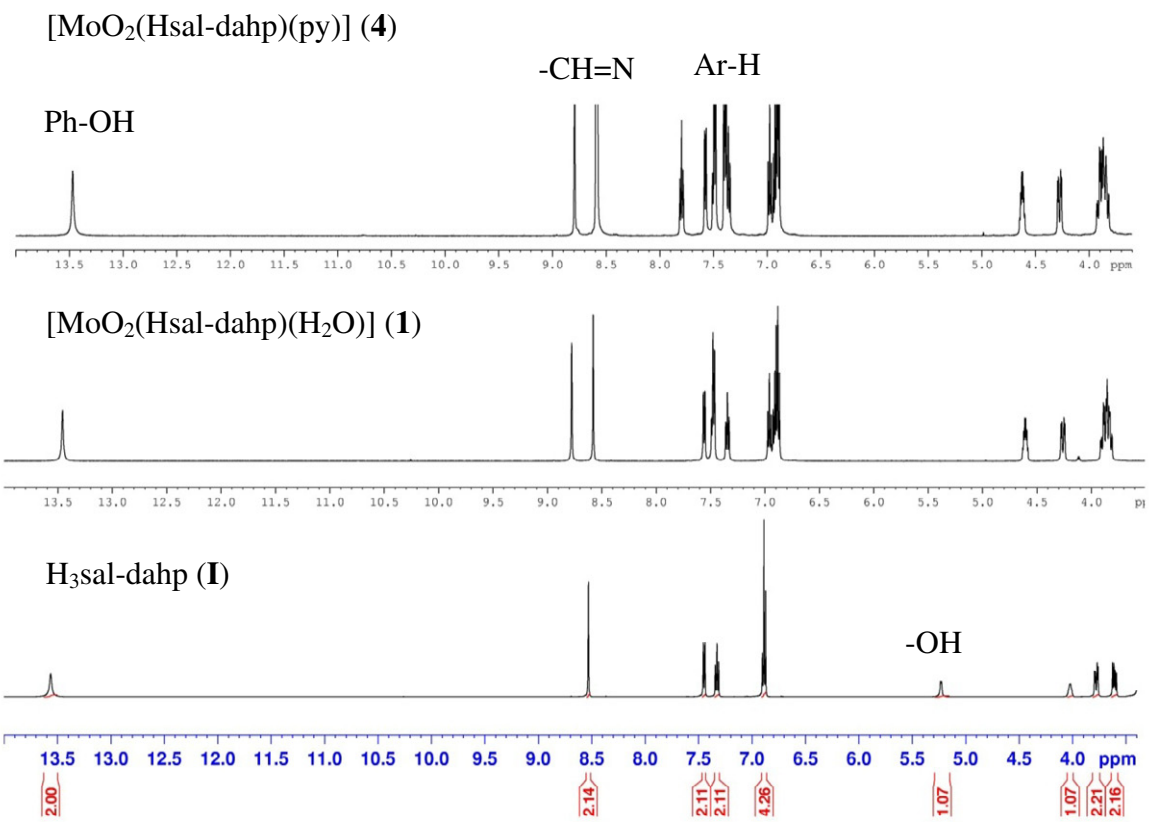

Fig. 5. ^{1}H NMR spectra of H_3sal-dahp (**I**), [MoO_2(Hsal-dahp)(H_2O)] (**1**) and [MoO_2(Hsal-dahp)(py)](**4**).

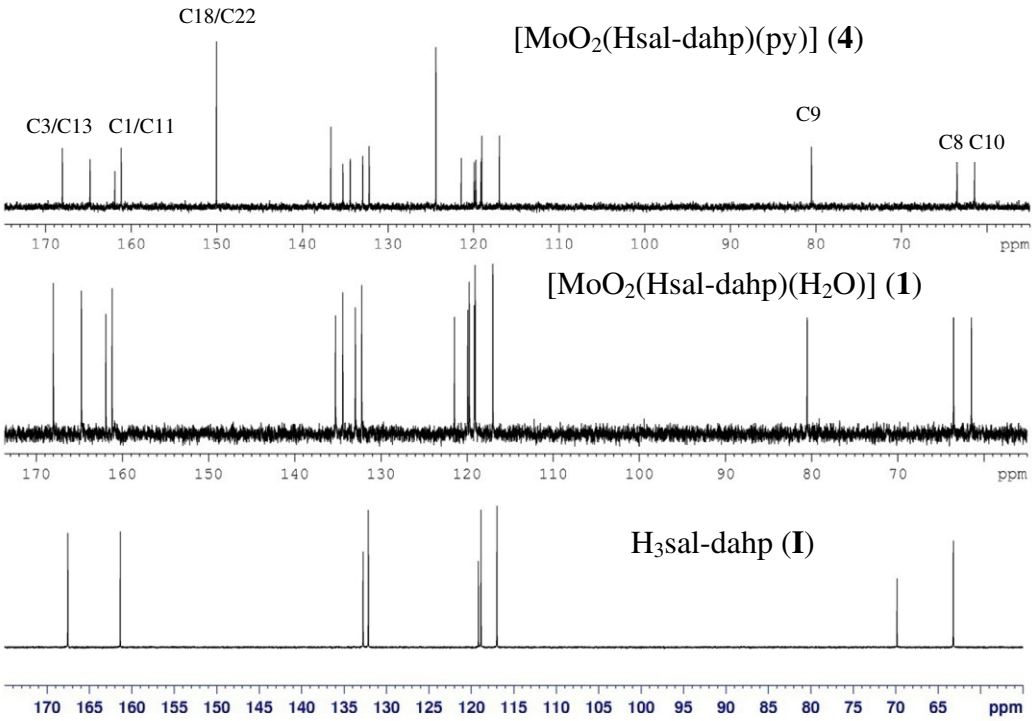

Fig. 6. ^{13}C NMR spectra of H_3sal-dahp (**I**), [MoO_2(Hsal-dahp)(H_2O)] (**1**) and [MoO_2(Hsal-dahp)(py)](**4**).

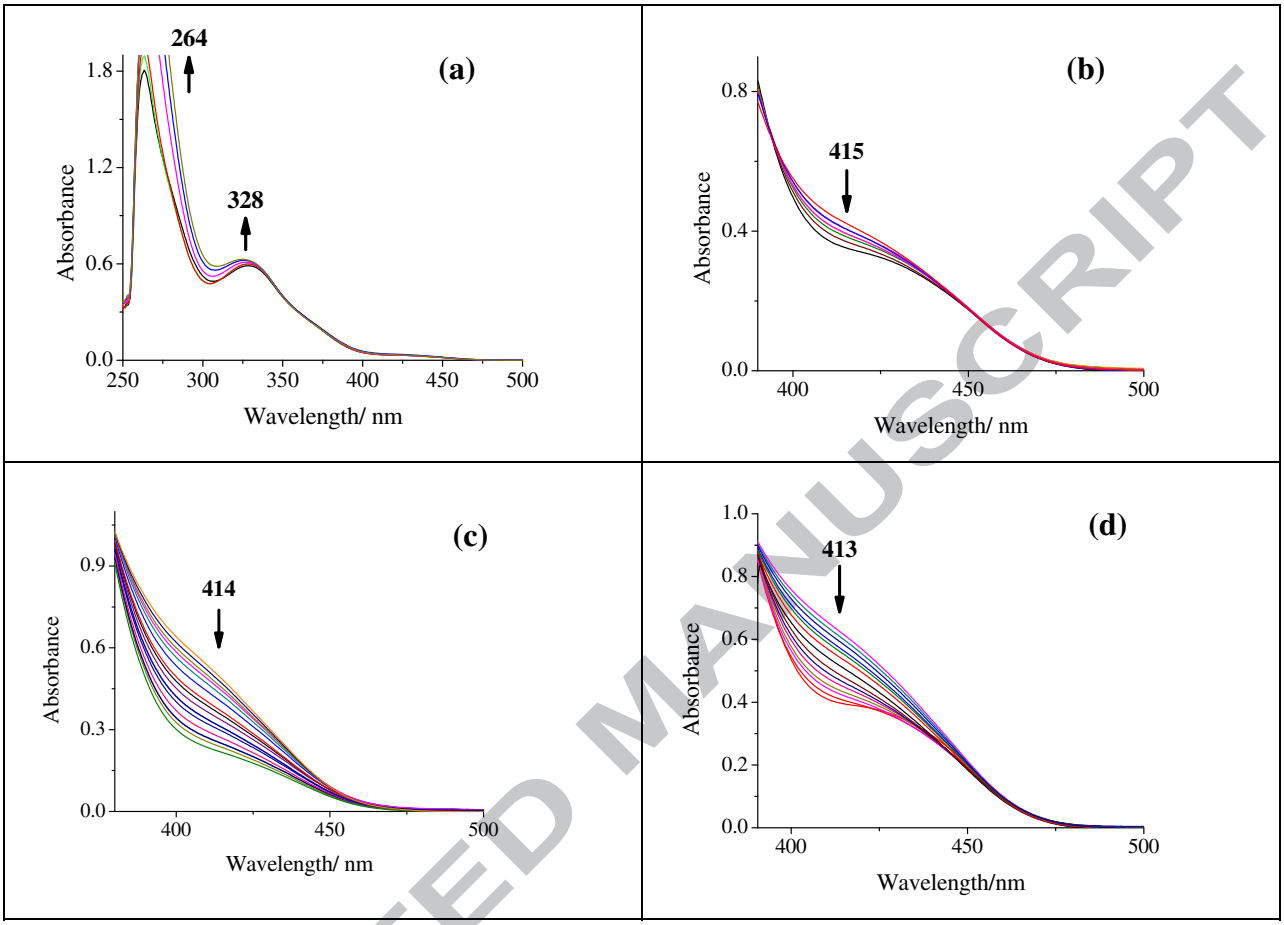

Fig. 7. Spectral changes observed during titration of dioxidomolybdenum(VI) complexes. (a) The spectra recorded after successive addition of one drop portions of 30% H_2O_2 (0.351 g, 3.1 mmol) dissolved in 5 mL (2.06 M) DMSO to 20 mL of a 6.7×10^{-5} M solution of [MoO_2(Hclsal-dahp)(H_2O)]. (b) The spectra recorded after successive addition of one drop portions of 30% H_2O_2 (0.253 g, 2.3 mmol) dissolved in 5 mL (1.48 M) DMSO to 15 mL of a 10^{-3} M solution of [MoO_2(Hclsal-dahp)(H_2O)]. (c) The spectra recorded after successive addition of one drop portions of 30% H_2O_2 (0.237 g, 2.10 mmol) dissolved in 5 mL (1.37 M) DMSO to 15 mL of a 10^{-3} M solution of [MoO_2(Hsal-dahp)(H_2O)]. (d) The spectra recorded after successive addition of one drop portions of 30% H_2O_2 (0.273 g, 2.4 mmol) dissolved in 5 mL (1.60 M) DMSO to 15 mL of a 10^{-3} M solution of [MoO_2(Hbrsal-dahp)(H_2O)].

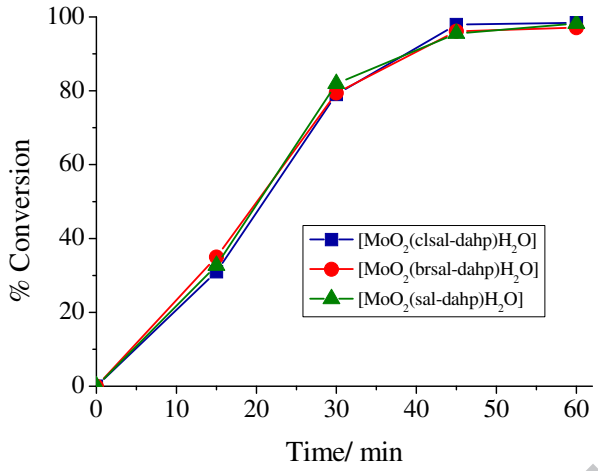

Fig. 8. Effect of different catalysts on the oxidative bromination of styrene.

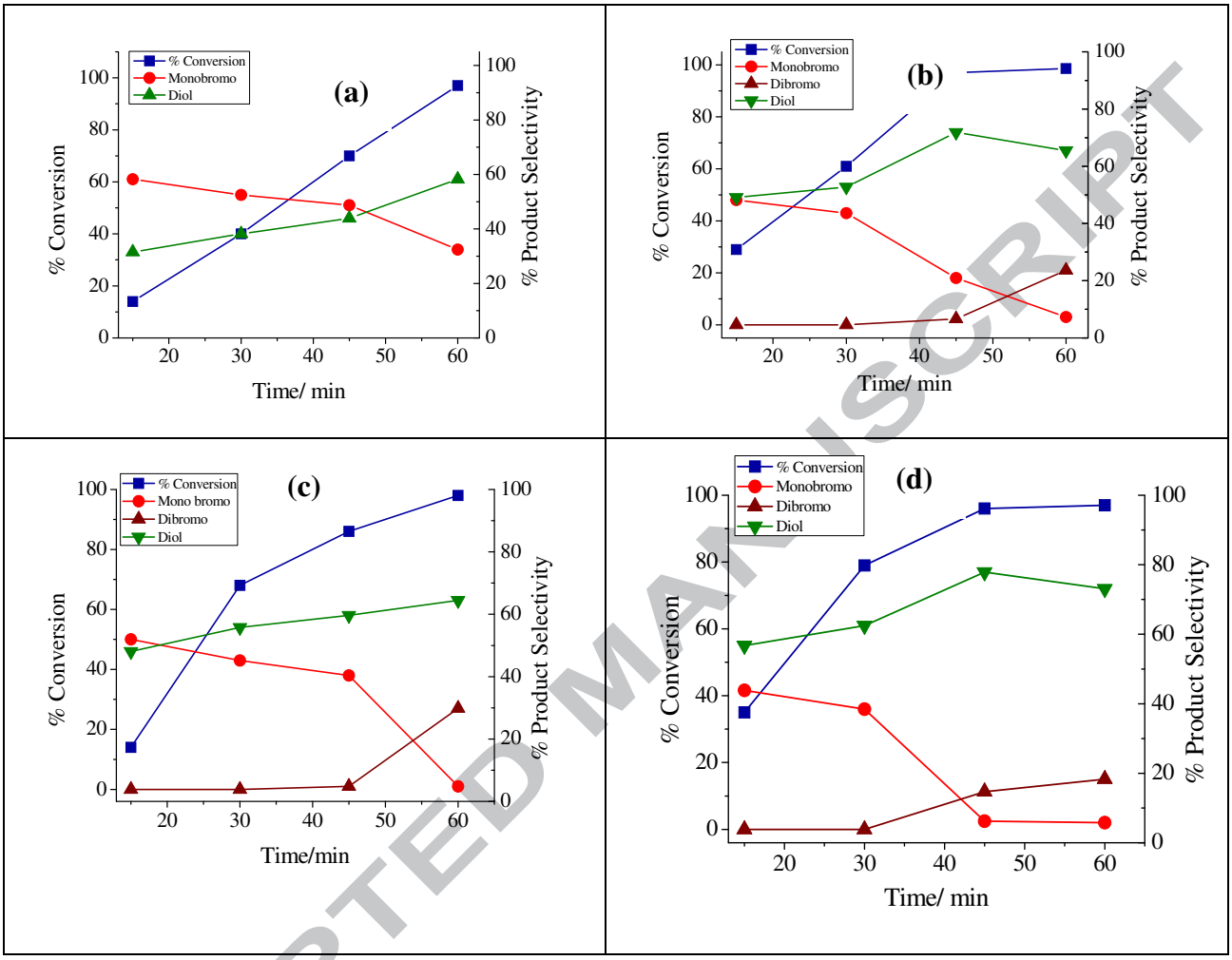

Fig. 9. Plots showing the percentage conversion of styrene and the selectivity of the formation of different reaction products as a function of time. (a) Reaction conditions: styrene (1.04 g, 10 mmol), [$Mo^{VI}O_2$(Hsal-dahp)(H_2O)] (**1**) (0.001g), 30 % aqueous H_2O_2 (2.27g, 20 mmol), KBr (2.38 g, 20 mmol) and 70 % aqueous $HClO_4$ (2.86 g, 20 mmol). (b) Reaction conditions: styrene (1.04 g,10 mmol), [$Mo^{VI}O_2$(Hsal-dahp)(H_2O)] (**1**) (0.001g), 30 % aqueous H_2O_2 (2.27 g, 20 mmol), KBr (2.38 g, 20 mmol) and 70 % aqueous $HClO_4$ (4.29 g, 30 mmol). (c) and (d) under conditions similar to (b) taking [$Mo^{VI}O_2$(Hclsal-dahp)(H_2O)] (**2**) and [$Mo^{VI}O_2$(Hbrsal-dahp)(H_2O)] (**3**), respectively as catalysts.

(b)

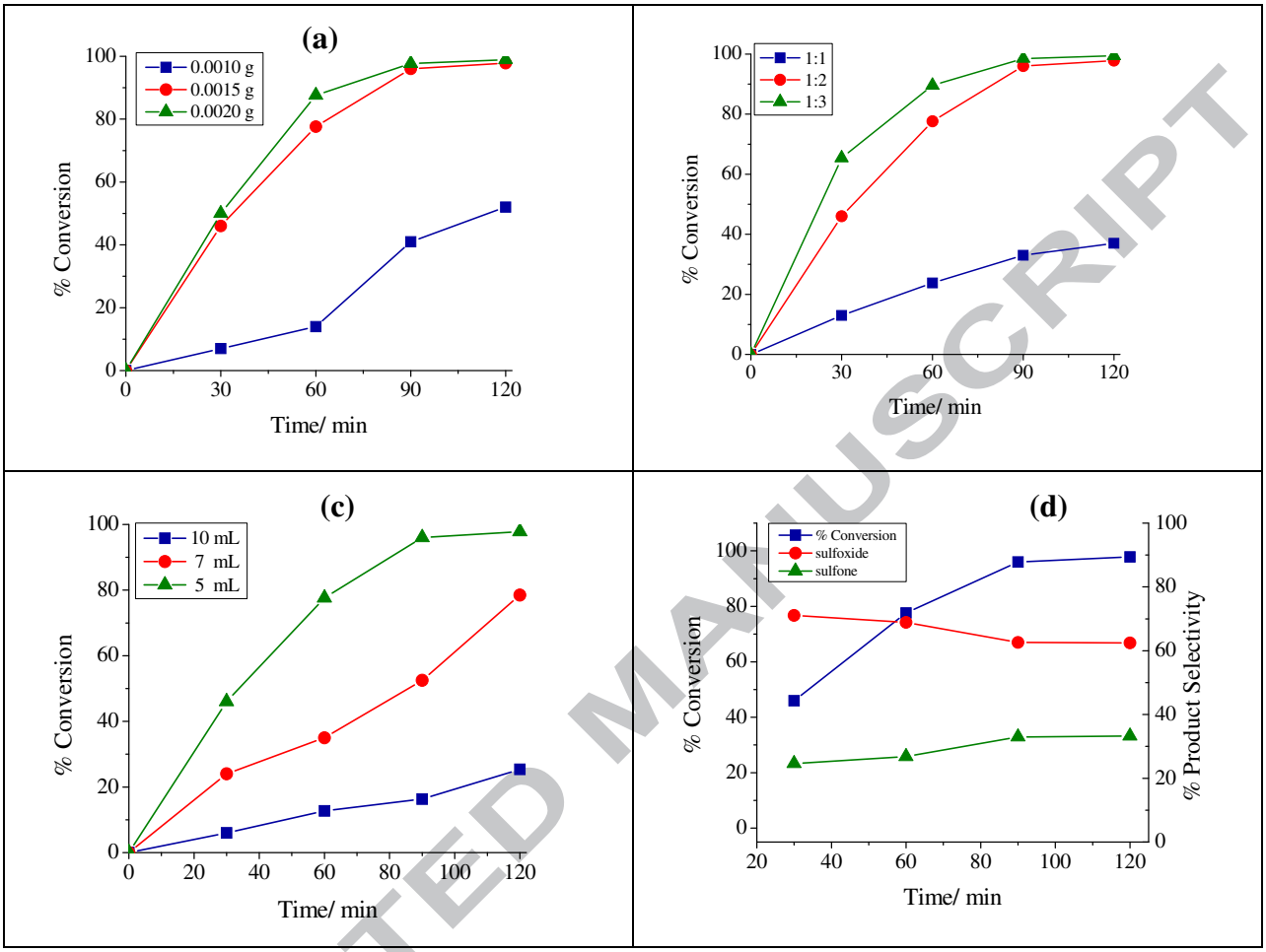

Fig. 10. (a) Effect of catalyst amount on the oxidation of methyl phenyl sulfide. Reaction conditions: methyl phenyl sulfide (1.24 g, 10 mmol), 30 % H_2O_2 (2.27 g, 20 mmol) and acetonitrile (5 mL). (b) Effect of oxidant amount on the oxidation of methyl phenyl sulfide. Reaction conditions: methyl phenyl sulfide (1.24 g, 10 mmol), catalyst (0.0015 g) and acetonitrile (5 mL). (c) Effect of solvent amount on the oxidation of methyl phenyl sulfide. Reaction conditions: methyl phenyl sulfide (1.24 g, 10 mmol), catalyst (0.0015 g) and 30 % H_2O_2 (2.27 g, 20 mmol). (d) Plot showing percentage conversion of methyl phenyl sulfide and the selectivity of the formation of methyl phenyl sulfoxide and methyl phenyl sulfone as a function of time under optimized conditions using [MoO_2(sal-dahp)(H_2O)] (**1**) as the catalyst.

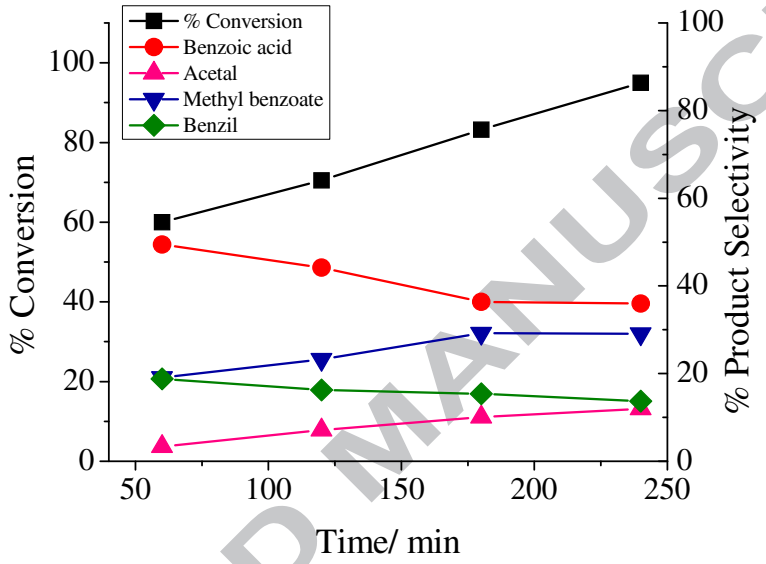

Fig. 11. Profiles showing percentage conversion of benzoin and the selectivity of the formation of benzoic acid, benzaldehyde-dimethylacetal, methyl benzoate and benzil as a function of time. Reaction condition: benzoin (1.06 g, 5 mmol), H_2O_2 (1.7 g, 15 mmol), [MoO_2(Hsal-dahp)H_2O] (0.0005 g) and methanol (10 mL) at reflux temperature.

Tables

Table 1

Crystal data and structure refinement parameters for [$Mo^{VI}O_2$(Hbrsal-dahp)(DMSO)] (**3a**) and [$Mo^{VI}O_2$(clsal-hdap)(DMSO)]$_4$[Mo_8O_{26}]·6DMSO (**7**).

	3a	**7**
Formula	$C_{19}H_{20}Br_2MoN_2O_6S$	$C_{60}H_{108}Cl_4Mo_{12}N_8O_{52}S_{10}$
Formula weight	660.19	3387.22
T/*K*	100(2)	100(2)
Wavelength/Å	0.71073	0.71073
Crystal system	Triclinic	Triclinic
Space group	P $\bar{1}$	P $\bar{1}$
a/Å	6.4781(11)	11.1756(3)
b/Å	12.819(2)	15.9726(5)
c/Å	14.330(3)	16.6625(5)
α/º	82.617(8)	109.950(2)
β/º	83.191(9)	102.650(2)
γ/º	75.476(8)	98.962(2)
V/Å^3	1137.7(3)	2640.40(13)
Z	2	1
F_{000}	648	1672
D_{calc}/g cm^{-3}	1.927	2.130
μ/mm^{-1}	4.218	1.766
θ/ (º)	1.44 to 28.02	1.36 - 28.80

R_{int}	0.1230	0.0638
Crystal size/mm^3	$0.47 \times 0.05 \times 0.05$	$0.160 \times 0.145 \times 0.050$
Goodness-of-fit on F^2	1.131	1.077
R_1 [a]	0.0683	0.0482
wR_2 (all data)[b]	0.1751	0.1497
Largest differences peak and hole/eÅ^{-3}	1.589 and -1.466	3.682 and -2.084

[a] $R_1 = \Sigma \left| \left| F_o \right| - \left| F_c \right| \right| / \Sigma \left| F_o \right|$. [b] $wR_2 = \{\Sigma[w(\left| \left| F_o \right|^2 - \left| F_c \right|^2 \right|)^2] / \Sigma[w(F_o^4)]\}^{1/2}$

Table 2

Bond lengths [Å] and angles [°] for [$Mo^{VI}O_2$(Hbrsal-dahp)(DMSO)] (**3a**) and [$Mo^{VI}O_2$(Hclsal-hdap)(DMSO)]$_4$[Mo_8O_{26}]·6DMSO (**7**).

Bond lengths	**7**	**3a**
Mo(1)-O(1)	1.947(6)	1.971(6)
Mo(1)-O(2)	1.922(4)	1.714(7)
Mo(1)-O(3C)	1.651(13)	Mo(1)-O(3) 1.714(6)
Mo(1)-O(3D)	1.713(13)	
Mo(1)-O(4)	1.683(5)	1.935(7)
Mo(1)-O(1D)	2.283(7)	2.303(6)
Mo(2)-O(5)	1.943(4)	
Mo(2)-O(6)	1.930(4)	
Mo(2)-O(7)	1.724(4)	
Mo(2)-O(8)	1.707(4)	
Mo(2)-O(2D)	2.270(4)	
Mo(1)-N(1)	2.268(6)	2.272(7)
Mo(2)-N(3)	2.270(5)	

Bond angles	**7**		**3a**
O(3C)-Mo(1)-O(4)	114.2(9)		
O(4)-Mo(1)-O(3D)	100.1(11)	O(3)-Mo(1)-O(4)	98.5(3)
O(3C)-Mo(1)-O(2)	110.6(10)	O(3)-Mo(1)-O(2)	105.8(3)
O(4)-Mo(1)-O(2)	99.1(2)	O(4)-Mo(1)-O(2)	98.7(3)

O(3D)-Mo(1)-O(2)	94.4(10)		
O(3C)-Mo(1)-O(1)	81.8(13)	O(3)-Mo(1)-O(1)	100.8(3)
O(4)-Mo(1)-O(1)	99.0(2)	O(4)-Mo(1)-O(1)	152.9(3)
O(3D)-Mo(1)-O(1)	104.4(13)		
O(2)-Mo(1)-O(1)	151.0(3)	O(2)-Mo(1)-O(1)	94.1(3)
O(3C)-Mo(1)-N(1)	83.8(9)	O(3)-Mo(1)-N(1)	162.6(3)
O(4)-Mo(1)-N(1)	161.9(3)	O(4)-Mo(1)-N(1)	75.3(3)
O(3D)-Mo(1)-N(1)	97.4(11)		
O(2)-Mo(1)-N(1)	74.94(19)	O(2)-Mo(1)-N(1)	91.2(3)
O(1)-Mo(1)-N(1)	80.8(2)	O(1)-Mo(1)-N(1)	80.7(3)
O(3C)-Mo(1)-O(1D)	154.2(13)	O(3)-Mo(1)-O(1D)	86.3(3)
O(4)-Mo(1)-O(1D)	85.9(3)	O(4)-Mo(1)-O(1D)	84.7(2)
O(3D)-Mo(1)-O(1D)	172.4(6)		
O(2)-Mo(1)-O(1D)	80.0(2)	O(2)-Mo(1)-O(1D)	166.6(3)
O(1)-Mo(1)-O(1D)	79.0(4)	O(1)-Mo(1)-O(1D)	77.9(2)
N(1)-Mo(1)-O(1D)	76.2(3)	N(1)-Mo(1)-O(1D)	77.1(3)
O(8)-Mo(2)-O(7)	106.5(2)		
O(8)-Mo(2)-O(6)	98.31(18)		
O(7)-Mo(2)-O(6)	96.92(19)		
O(8)-Mo(2)-O(5)	101.55(18)		
O(7)-Mo(2)-O(5)	95.48(19)		
O(6)-Mo(2)-O(5)	152.49(17)		
O(8)-Mo(2)-O(2D)	86.80(18)		
O(7)-Mo(2)-O(2D)	166.41(18)		
O(6)-Mo(2)-O(2D)	83.48(15)		

O(5)-Mo(2)-O(2D)	78.84(15)
O(8)-Mo(2)-N(3)	163.27(19)
O(7)-Mo(2)-N(3)	89.72(19)
O(6)-Mo(2)-N(3)	75.24(16)
O(5)-Mo(2)-N(3)	80.37(15)
O(2D)-Mo(2)-N(3)	77.21(15)

Table 3
Mo-O bond distances for the β isomer of $[Mo_8O_{26}]^{4-}$

$Mo\text{-}O_t$		
	Mo(5)-O(9)	1.703(4)
	Mo(4)-O(16)	1.688(4)
	Mo(6)-O(17)	1.707(4)
	Mo(3)-O(18)	1.693(4)
	Mo(4)-O(19)	1.708(4)
	Mo(6)-O(20)	1.697(4)
	Mo(5)-O(21)	1.713(4)
$Mo\text{-}O_{2c}$		
	Mo(4)-O(11)	1.927(4)
	Mo(6)-O(11)	1.895(4)
	Mo(4)-O(14)	1.935(3)
	Mo(5)-O(14)	1.883(4)
	Mo(3)-O(15)	1.744(4)
	Mo(4)-O(15)	2.291(4)
$Mo\text{-}O_{3c}$		
	Mo(3)-O(10)	1.958(4)
	Mo(5)-O(10)#1	1.994(4)
	Mo(6)-O(10)	2.318(3)
	Mo(3)-O(12)#1	1.942(3)

	Mo(5)-O(12)#1	2.322(3)
	Mo(6)-O(12)	2.013(3)
$Mo\text{-}O_{5c}$		
	Mo(3)-O(13)	2.331(3)
	Mo(3)-O(13)#1	2.145(4)
	Mo(4)-O(13)	2.461(4)
	Mo(5)-O(13)	2.323(4)
	Mo(6)-O(13)	2.333(4)

Symmetry transformations used to generate equivalent atoms: #1 -x+1,-y,-z+1

Table 4

IR spectral data [in cm^{-1}] of the compounds

Compounds	ν(C=$N_{azomethine}$/ N_{ring})	ν_{asym}(O=Mo=O)	ν_{sym}(O=Mo=O)
H_3sal-dahp (**I**)	1633		
H_3clsal-dahp (**II**)	1638		
H_3brsal-dahp (**III**)	1638		
[$Mo^{VI}O_2$(sal-dahp)(H_2O)] (**1**)	1644, 1603	918	890
[$Mo^{VI}O_2$(clsal-dahp)(H_2O)] (**2**)	1650, 1598	918	892
[$Mo^{VI}O_2$(brsal-dahp)(H_2O)] (**3**)	1649, 1598	914	889
[$Mo^{VI}O_2$(sal-dahp)(py)] (**4**)	1650, 1597	928	903
[$Mo^{VI}O_2$(clsal-dahp)(py)] (**5**)	1652, 1639	917	903
[$Mo^{VI}O_2$(brsal-dahp)(py)] (**6**)	1654, 1638	921	902

Table 5

Electronic spectral data of the ligands and the complexes.

Compound	Solvent	λ_{max} [nm]
H_3sal-dahp (**I**)	MeOH	217 (2.8×10^4), 256 (1.3×10^4), 279 (4.6×10^3), 317 (4.5×10^3)
H_3clsal-dahp (**II**)	MeOH	223 (5×10^4), 256 (8.2×10^3), 277 (1.9×10^3), 327 (2.8×10^3)
H_3brsal-dahp (**III**)	MeOH	225 (7.2×10^4), 254 (2.5×10^4), 279 (6.6×10^3), 329 (8.4×10^3)
$[Mo^{VI}O_2$(sal-dahp)$(H_2O)]$ (**1**)	DMSO	263 (3.8×10^4), 321 (7.7×10^3), 414 (0.3×10^3)
$[Mo^{VI}O_2$(clsal-dahp)$(H_2O)]$ (**2**)	DMSO	264 (2.6×10^4), 328 (9×10^3), 415 (0.3×10^3)
$[Mo^{VI}O_2$(brsal-dahp)$(H_2O)]$ (**3**)	DMSO	263 (4.7×10^4), 329 (1.5×10^4), 413 (0.4×10^3)
$[Mo^{VI}O_2$(sal-dahp)(py)] (**4**)	DMSO	263 (2.6×10^4), 321 (7.5×10^3), 430 ($0.5\times$ v10^3)
$[Mo^{VI}O_2$(clsal-dahp)(py)] (**5**)	DMSO	260 (2.1×10^4), 329 (6.8×10^3), 430 (0.5×10^3)
$[Mo^{VI}O_2$(brsal-dahp)(py)] (**6**)	DMSO	259 (2.1×10^4), 329 (6.2×10^3), 431 (0.5×10^3)

Table 6

^{1}H NMR chemical shifts [δ in ppm] of the ligands and the complexes recorded in DMSO-d_6.

Compo-und[a, b]	–OH (phenolic)	–OH (alcoholic)	–CH=N–	Aliphatic protons -CH	-CH_2	Aromatic protons
I	13.56 (br, 2H)	5.24 (br, 1H)	8.54 (s, 2H)	4.03 (m, 1H)	3.77 (dd, 2H), 3.56 (m, 2H)	7.47-6.90 (m, 8H)
II	13.56 (br, 2H)	5.24 (br, 1H)	8.54 (s, 2H)	4.03 (m, 1H)	3.77 (dd, 2H), 3.56 (m, 2H)	7.47-6.90 (m, 8H)
III	13.56 (br, 2H)	5.24 (br, 1H)	8.54 (s, 2H)	4.03 (m, 1H)	3.77 (dd, 2H), 3.56 (m, 2H)	7.47-6.90 (m, 8H)
1	13.45 (br, 1H)		8.54 (s, 1H), 8.79 (s, 1H)	4.65 (m, 1H)	4.29 (dd, 2H), 3.88 (m, 2H)	7.65-6.90 (m, 8H)
$\Delta\delta$			(0.25)	(0.62)		
2	13.45 (br, 1H)		8.54 (s, 1H), 8.79 (s, 1H)	4.65 (m, 1H)	4.29 (dd, 2H), 3.88 (m, 2H)	7.65-6.90 (m, 8H)
$\Delta\delta$			(0.25)	(0.62)		
3	13.45 (br, 1H)		8.54 (s, 1H), 8.79 (s, 1H)	4.65 (m, 1H)	4.29 (dd, 2H), 3.88 (m, 2H)	7.65-6.90 (m, 8H)
$\Delta\delta$			(0.25)	(0.62)		
4	13.45 (br, 1H)		8.54 (s, 1H), 8.79 (s, 1H)	4.65 (m, 1H)	4.29 (dd, 2H), 3.88 (m, 2H)	7.65-6.90 (m, 8H)
$\Delta\delta$			(0.25)	(0.62)		
5	13.45 (br, 1H)		8.54 (s, 1H), 8.79 (s, 1H)	4.65 (m, 1H)	4.29 (dd, 2H), 3.88 (m, 2H)	7.65-6.90 (m, 8H)
$\Delta\delta$			(0.25)	(0.62)		
6	13.45 (br, 1H)		8.54 (s, 1H), 8.79 (s, 1H)	4.65 (m, 1H)	4.29 (dd, 2H), 3.88 (m, 2H)	7.65-6.90 (m, 8H)
$\Delta\delta$			(0.25)	(0.62)		

[a]Letters given in parentheses indicate the signal structure: s = singlet, dd = doublet of doublet, q = quartet, m = multiplet, br = broad (unresolved).
[b]Coordination induced shifts $\Delta\delta$ = [δ(complex) – δ(free ligand)]

Table 7

^{13}C NMR spectral data of the ligand and the complexes

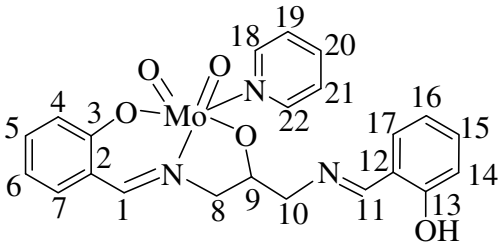

Compound	C1, C11	C3, C13	C9	C8, C10	C2, C12,	C4–C7, C14–C17	C18–C22
I	161.3	167.5	69.8	63.2	132.7	117,132,118,119,	
II	160.5	166.4	69.5	62.9	132.5	119,131,120,122,	
III	161.0	166.3	69.5	62.8	135.2	109,133,119,120	
1 (Δδ)	160.7, 161.4	164.2, 167.5	80.0 (10.2)	60.9, 63.0	133, 134,	118.6,131.7,119.4,120. 9, 118.5,132.4,119.2,116.5	
2 (Δδ)	160.2, 160.7	163.8, 166.7	80.5 (11.0)	61.2, 63.6	133, 134,	119,131,120,122, 121,132.6,122.5,123	
3 (Δδ)	160.7, 161.2	163.8, 166.6	80.5 (11.0)	61.2, 63.6	136, 137,	109,133,119,120, 110,135,122,123	
4 (Δδ)	161.0, 162.0	164.7, 168	80.5 (10.7)	61.4, 63.5	134, 135	119.1,132,119.9,121, 119,133,119.7,117	150.0,136.6, 124.4
5 (Δδ)	160.2, 160.8	163.9, 166.7	80.5 (11.0)	61.2, 63.6	133, 134.7,	119,131,121,122, 120,132.6,122.5,123	150.0,136.6, 124.4
6 (Δδ)	160.3, 160.7	163.4, 166.2	80.1 (10.6)	60.7, 63.1	135.6, 137,	109,133.5,119,121, 109.8,135,120.3,122.7	149.6,136.2,124

Table 8

Conversion of styrene (1.04 g, 10 mmol), TOF and product selectivity using [$Mo^{VI}O_2$(Hsal-dahp)(H_2O)] as a catalyst precursor in 1 h of reaction time under different reaction conditions.

Entry No.	KBr [g (mmol)]	H_2O_2 [g (mmol)]	$HClO_4$ [g (mmol)]	Catalyst [g (mmol)]	Conv. [%]	TOF [h^{-1}]	Mono Bromo	Dibromo	Diol	Other product
1.	3.57 (30)	3.39 (30)	5.72 (40)	0.001 (2.2×10^{-3})	98	4454	0.1	39.9	52	8
2	3.57 (30)	3.39 (30)	5.72 (40)	0.0015 (3.4×10^{-3})	98	2882	0.2	27.4	63.4	9
3	3.57 (30)	3.405 (30)	5.72 (40)	0.002 (4.5×10^{-3})	99	2200	0.4	26	67.6	6
4	3.57 (30)	2.27 (20)	5.72 (40)	0.001 (2.2×10^{-3})	97	4409	15	9.2	69.8	6
5	3.57 (30)	4.52 (40)	5.72 (40)	0.001 (2.2×10^{-3})	98	4454	0.6	21.4	66	12
6	2.38 (20)	2.27 (20)	5.72 (40)	0.001 (2.2×10^{-3})	98	4454	26	28	41	5
7	4.76 (40)	2.27 (20)	5.72 (40)	0.001 (2.2×10^{-3})	99	4500	0.3	32	55.7	12
8	2.38 (20)	2.27 (20)	2.86 (20)	0.001 (2.2×10^{-3})	97	4409	34	0	61	5
9	2.38 (20)	2.27 (20)	4.29 (30)	0.001 (2.2×10^{-3})	98	4454	3	21	67	9
10[a]	2.38 (20)	2.27 (20)	4.29 (30)	0.001 (1.9×10^{-3})	98	5157	1	27	63	9
11[b]	2.38 (20)	2.27 (20)	4.29 (30)	0.001 (1.6×10^{-3})	97	6062	2	15	72	11
12.	2.38 (20)	2.27 (20)	2.86 (20)	blank	44	-	45	0	52	3
13.	2.38 (20)	2.27 (20)	4.29 (30)	blank	60	-	39	0	58	3

[a]Data for[$Mo^{VI}O_2$(clsal-dahp)(H_2O)].

[b]Data for [$Mo^{VI}O_2$(brsal-dahp)(H_2O)].

Table 9

Oxidation of methyl phenyl sulfide, TOF and product selectivity using the molybdenum complexes as catalysts.

Catalyst [g (mmol)]	TOF [h^{-1}][a]	Conv. [%]	Selectivity [%][b]	
			sulfoxide	sulfone
[MoO_2(Hsal-dahp)(H_2O)] (**1**) [0.0015 (3.4×10^{-3})]	1441	98	66.8	33.2
[MoO_2(Hclsal-dahp)(H_2O)] (**2**) [0.0015 (2.9×10^{-3})]	1672	97	68	32
[MoO_2(Hbrsal-dahp)(H_2O)] (**3**) [0.0015 (2.5×10^{-3})]	1920	96	70	30
Blank reaction	-	20	79	21

[a]TOF values calculated at 2 h of reaction time.
[b]sulfoxide; methyl phenyl sulfoxide; sulfone: methyl phenyl sulfone.

Table 10

Conversion of benzoin (1.06 g, 5 mmol) using [MoO_2(sal-dahp)(H_2O)] (**1**) as a catalyst in 4 h of reaction time under different reaction conditions.

Entry No.	Catalyst [g (mmol)]	H_2O_2 [g (mmol)]	CH_3OH [mL]	Conv. [%]
1	0.0005 (1.1×10^{-3})	1.14 (10)	10	83
2	0.0005 (1.1×10^{-3})	1.71 (15)	10	95
3	0.0005 (1.1×10^{-3})	2.27 (20)	10	97
4	0.0005 (1.1×10^{-3})	1.71 (15)	15	88
5	0.0005 (1.1×10^{-3})	1.71 (15)	20	86
6	0.0010 (2.2×10^{-3})	1.71 (15)	10	96
7	0.0015 (3.4×10^{-3})	1.71 (15)	10	97

Table 11

Effect of different catalysts on the oxidation of benzoin, TOF and product selectivity.

Catalyst [g (mmol)]	TOF [h^{-1}][a]	Conv. [%]	Selectivity [%][b]			
			a	b	c	d
[MoO_2(Hsal-dahp)(H_2O)] (**1**) [0.0005 (1.1×10^{-3})]	1080	95	40	13	32	15
[MoO_2(Hclsal-dahp)(H_2O)] (**2**) [0.0005 (0.97×10^{-3})]	1213	97	49	10	30	11
[MoO_2(Hbrsal-dahp)(H_2O)] (**3**) [0.0005 (0.83×10^{-3})]	1446	96	41	11	30	18

[a]TOF values calculated at 4 h of reaction time.

[b]See scheme 6 for details of products.

Supporting information

Potential pentadentate ligands behaving as tridentate: Synthesis, characterization and catalytic activity of dioxidomolybdenum(VI) complexes

Mannar R. Maurya, Sarita Dhaka, Fernando Avecilla

Table S1

Conversion of methyl phenyl sulfide (1.24 g, 10 mmol) using $[MoO_2(sal\text{-}dahp)(H_2O)]$ (**1**) as a catalyst in 2 h of reaction time under different reaction conditions.

Entry No.	Catalyst [g (mmol)]	H_2O_2 [g (mmol)]	CH_3CN [mL]	Conv. [%]
1	0.0015 (3.3×10^{-3})	1.14 (10)	5	37
2	0.0015 (3.3×10^{-3})	2.27 (20)	5	98
3	0.0015 (3.3×10^{-3})	3.39 (30)	5	99
4	0.0015 (3.3×10^{-3})	2.27 (20)	7	78
5	0.0015 (3.3×10^{-3})	2.27 (20)	10	25
6	0.001 (2.2×10^{-3})	2.27 (20)	05	52
7	0.002 $((4.4 \times 10^{-3})$	2.27 (20)	15	99

IR spectral study

IR spectra of a representative ligand and complex are presented in Fig. S1.

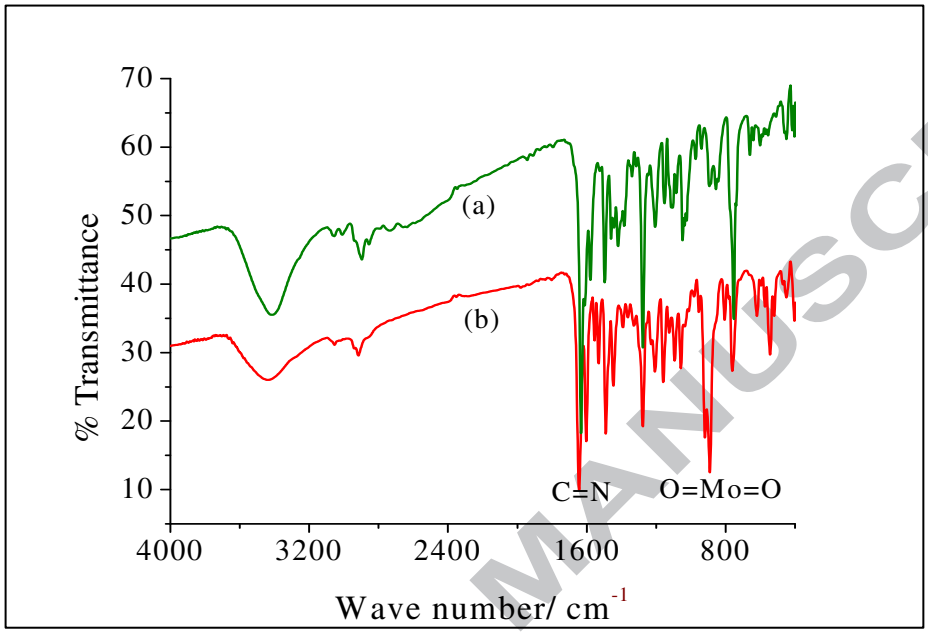

Fig. S1. IR spectra of H_3sal-dahp (a) and [$Mo^{VI}O_2$(Hsal-dahp)(H_2O)] (b).

Oxidation of methyl phenyl sulfide

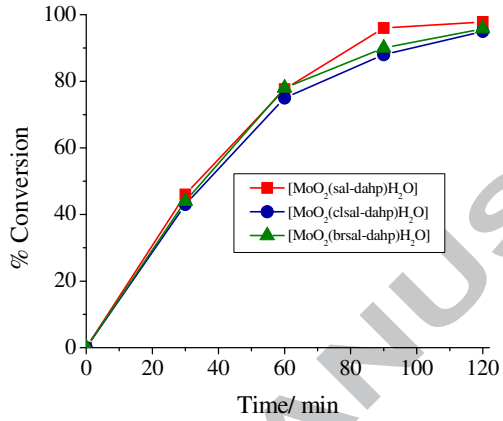

Fig. S2. Effect of different catalysts on the oxidation of methyl phenyl sulfide.

Oxidation of benzoin

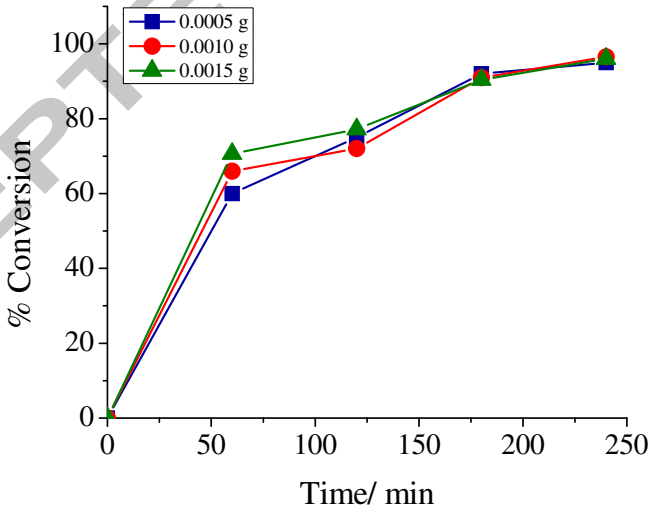

Fig. S3. Effect of catalyst amount on the oxidation of benzoin. Reaction conditions: benzoin (1.06 g, 5 mmol), 30 % H_2O_2 (1.7 g, 15 mmol) and methanol (10 mL).

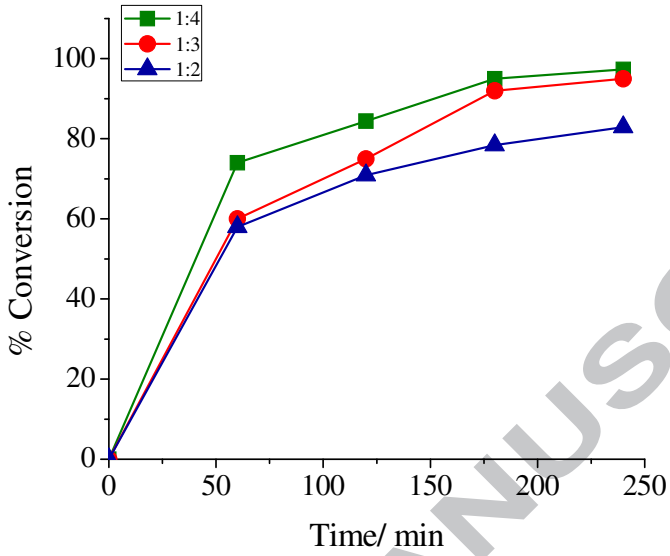

Fig. S4. Effect of oxidant amount on the oxidation of benzoin. Reaction conditions: benzoin (1.06 g, 5 mmol), catalyst amount (0.0005 g) and methanol (10 mL).

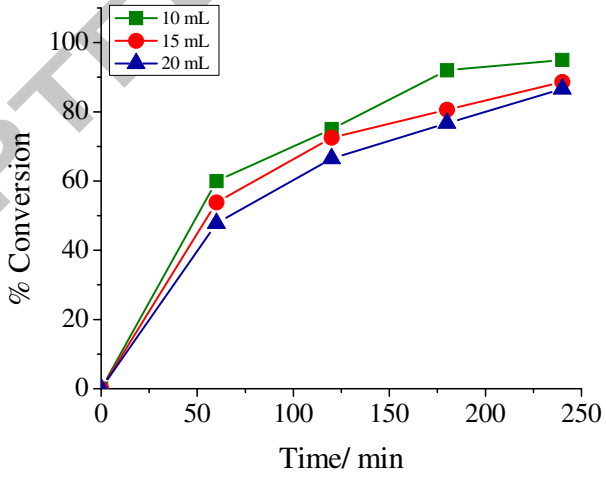

Fig. S5. Effect of solvent amount on the oxidation of benzoin. Reaction conditions: benzoin (1.06 g, 5 mmol), catalyst amount (0.0005 g) and 30% H_2O_2 (1.7 g, 15 mmol).

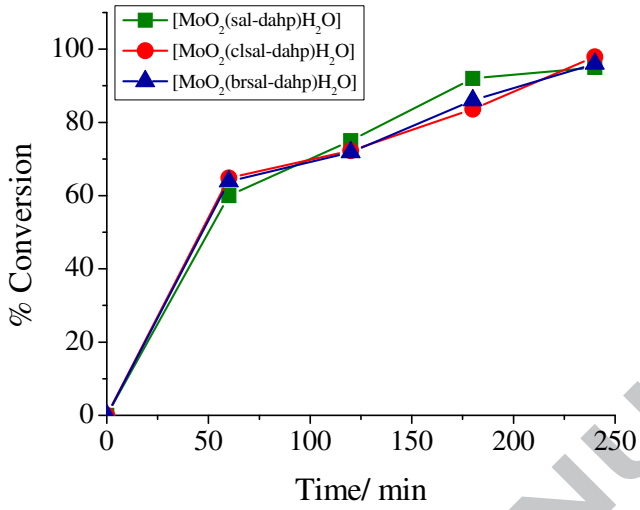

Fig. S6. Effect of various catalysts on the oxidation of benzoin. Reaction conditions: benzoin (1.06 g, 5 mmol), 30% H_2O_2 (1.7 gm, 15 mmol), catalyst amount (0.0005 gm) and methanol (10 mL).

(Graphical Abstract)

Synthesis, characterization and catalytic activity of dioxidomolybdenum(VI) complexes of tribasic pentadentate ligands

M. R. Maurya, S. Dhaka, F. Avecilla

Dioxidomolybdenum(VI) complexes of tribasic pentadentate ligands have been isolated and characterized. Their catalytic activities for the oxidative bromination of styrene and the oxidation of methyl phenyl sulfide and benzoin are reported.

(Graphical Abstract)

Synthesis, characterization and catalytic activity of dioxidomolybdenum(VI) complexes of tribasic pentadentate ligands

M. R. Maurya, S. Dhaka, F. Avecilla

Dioxidomolybdenum(VI) complexes of tribasic pentadentate ligands have been isolated and characterized. Their catalytic activities for the oxidative bromination of styrene and the oxidation of methyl phenyl sulfide and benzoin are reported.